Chemical Science

ROYAL SOCIETY OF CHEMISTRY

PERSPECTIVE

View Article Online
View Journal | View Issue

Cite this: *Chem. Sci.*, 2026, **17**, 5297

All publication charges for this article have been paid for by the Royal Society of Chemistry

Received 14th September 2025
Accepted 1st February 2026

DOI: 10.1039/d5sc07076g

rsc.li/chemical-science

Far-field single-molecule vibrational spectroscopy and imaging

Philip A. Kocheril, [a] Haomin Wang, [a] Ryan E. Leighton, [a] Dongkwan Lee,[a] Noor Naji, [a] Wei Min [b] and Lu Wei *[a]

Single-molecule (SM) optical spectroscopy and imaging approaches have proven transformative, allowing for deep insights into molecular dynamics and behaviour. Despite their intrinsically weaker signals, vibrational spectro-microscopies have advanced significantly within the past decade, allowing for far-field vibrational spectroscopy and imaging at the SM level under ambient conditions. In this Perspective, we first discuss the critical insights and advancements that allowed for SM vibrational spectroscopy and imaging to be realized, highlighting the technical developments that have allowed vibrational spectro-microscopies to break the SM barrier with far-field optics. We then discuss the unique and exciting opportunities of these SM vibrational methods.

1. Introduction

Since the first optical single-molecule (SM) detection in 1989, SM spectroscopy has proven revolutionary over the past 36 years.[1–5] Bulk spectroscopic techniques report ensemble-averaged observables from many molecules, obscuring the unique behaviours of individual molecules. By studying one molecule at a time, SM spectroscopy has offered us the unprecedented capability to investigate the intrinsic heterogeneity of molecular properties without ensemble averaging, allowing direct visualization of transient dynamics and the ability to quantify distributions rather than means.[6]

SM spectroscopy has allowed paradigm-shifting insights from spectral diffusion,[3] molecular orientation,[7] and molecular motion[8] to SM protein biophysics,[9] SM biomechanics,[10] SM cell biology,[11,12] and super-resolution microscopy.[13] For instance, video-rate fluorescence imaging of the rotating γ-subunit of F_1-ATPase enabled direct quantification of kinetics and dynamics at the single-protein level.[14] Additionally, protein folding studies have been transformed by SM Förster resonance energy transfer (smFRET)[15,16] allowing for direct probing of protein folding even under non-equilibrium conditions.[17] Furthermore,

[a]*Division of Chemistry and Chemical Engineering, California Institute of Technology, Pasadena, CA 91125, USA. E-mail: lwei@caltech.edu*
[b]*Department of Chemistry, Columbia University, New York, NY 10027, USA*

Philip A. Kocheril

Philip Kocheril received his BS in Specialized Chemistry from the University of Illinois at Urbana-Champaign in 2021. Starting from high school, Phil worked with Prof. Benjamin McCall, performing ultraprecise gas-phase infrared spectroscopy, and later worked with Prof. Steven Zimmerman on drug discovery for myotonic dystrophy type 1. He was also a post-bachelor's student at Los Alamos National Laboratory, developing waveguide-based biosensors and synthetic lipoproteins. Phil is currently a Hertz Fellow, an NSF Graduate Research Fellow, and a PhD candidate in Prof. Lu Wei's group, focusing on integrating spectroscopy and computation to deepen molecular understanding and develop tools for vibrational bioimaging.

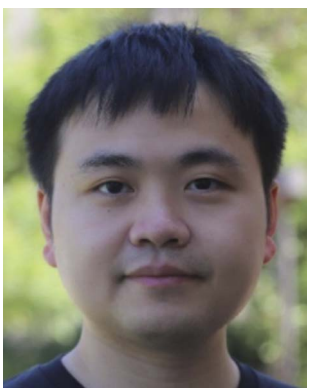

Haomin Wang

Haomin Wang received his BS from Peking University in 2015 and his PhD from Lehigh University in 2020 under the supervision of Prof. Xiaoji Xu. He conducted postdoctoral research with Prof. Wei from 2020 to 2025. He is currently an Assistant Professor in the Department of Chemistry at Fudan University, China. His research focuses on the development of advanced vibrational spectro-microscopy instrumentation and methodologies. He was awarded the ACS PHYS Young Investigator Award in 2025.

SM sensitivity is the foundation of SM localization microscopy (SMLM),[18] a class of super-resolution optical microscopy methods that provide extremely high resolution (even down to the Å level) in imaging biological systems.[19]

Complementary to these fluorescence-based methods, vibrational spectroscopy, based on either infrared (IR) absorption or Raman scattering, which have complementary vibrational selection rules, has the potential to address some fundamental challenges faced by fluorescence and offer complementary and fundamentally new understandings of molecular behaviours and interactions.[20,21] Due to operating on different fundamental principles than fluorescence, vibrational spectroscopies provide unique opportunities, including: first, use of bioorthogonal vibrational tags. Rather than tagging with fluorescent proteins or molecular fluorophores (which may perturb the dynamics of the tagged species), vibrational spectromicroscopies can leverage much smaller chemical tags, such as alkynes (–C≡C–),[22] nitriles (–C≡N),[23] and deuterium labelling (–C–D),[24] or even operate entirely without exogenous labels.[20] Vibrational tags also do not generally suffer from photobleaching, allowing for more straightforward quantitation in absolute concentrations.[25] Second, vibrational imaging facilitates the simultaneous visualization of many different targets in a single shot, due to the intrinsically narrow linewidths of

Ryan E. Leighton

Ryan Leighton received his BS in Chemistry and BA in Physics in 2018 from the University of Minnesota – Duluth, working under Prof. Ahmed Heikal and Prof. Erin Sheets, to characterize FRET sensors. He received his PhD in Chemistry in 2023 from the University of Minnesota – Twin Cities in Prof. Renee Frontiera's lab, focusing on the development of super-resolution stimulated Raman microscopy. He joined Prof. Wei's lab at Caltech as a postdoc in 2024 and was awarded the 2025 Arnold O. Beckman Postdoctoral Fellowship in Chemical Instrumentation. His research involves developing novel nonlinear vibrational microscopy methods.

Dongkwan Lee

Dongkwan Lee earned his BS in Chemical Engineering from the University of Illinois at Urbana-Champaign, where he worked with Prof. Rohit Bhargava and Prof. Ryan Bailey. Dongkwan earned his PhD from Caltech in 2025 and continued as a postdoctoral scholar with Prof. Wei, focusing on pushing the fundamental limits of optical microscopy for chemical imaging.

Noor Naji

Noor Naji received her BS in chemistry from California State Polytechnic University, Pomona in 2022, where she worked in Prof. Gregory Barding's bioanalytical chemistry lab. She is currently pursuing her PhD at Caltech in Prof. Wei's lab, focusing on applying spectromicroscopy tools for local sensing in biology.

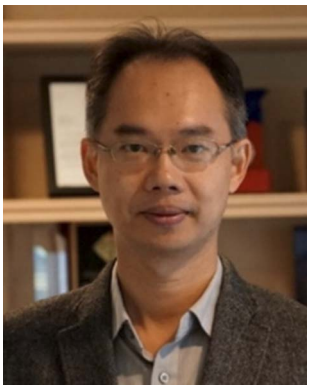

Wei Min

Wei Min received his BS from Peking University in 2003 and PhD from Harvard University in 2008 studying single-molecule biophysics with Prof. Sunney Xie. After continuing his postdoctoral work in the Xie group, Wei joined the faculty at Columbia University in 2010 and was promoted to Full Professor in 2017. Wei has been recognized by a number of honors, including the SPIE Biophotonics Technology Innovator Award (2023), the Craver Award of Vibrational Spectroscopy (2022), the Scientific Achievement Award from Royal Microscopical Society (2021), the Pittsburgh Conference Achievement Award (2019) and the ACS Early Career Award in Experimental Physical Chemistry (2017).

Lu Wei

Lu Wei received her BS from Nanjing University in 2010 and obtained her PhD from Columbia University in 2015, working with Prof. Wei Min. Too fascinated by stimulated Raman scattering microscopy, she stayed at Columbia as a postdoctoral scholar, continuing to develop new nonlinear vibrational imaging techniques. Lu joined the faculty at Caltech in 2018 and was promoted to Professor of Chemistry in 2025. Lu is a Heritage Medical Research Institute investigator and Ronald and JoAnn Willens Scholar at Caltech. Lu has recently received several honors, including the Camille Dreyfus Teacher-Scholar Award (2025), Coblentz Award (2025), the NSF CAREER Award (2023), the Sloan Research Fellowship (2022), and the NIH Director's New Innovator Award (2020).

vibrational spectra.[26,27] Third, vibrational spectroscopic observables can be used to quantitatively obtain rich chemical information with physical interpretability,[28,29] made possible by robust connections between first-principles theory and experiments.[30,31] Despite these benefits and more, vibrational spectro-microscopies have historically been limited in scope, due to poorer intrinsic sensitivity than fluorescence-based methods.

To enable SM detection, ideally a method needs to fulfil both of the following criteria:

(1) large cross-sections, and

(2) detection schemes with minimal noise and background.

Fluorescence-based methods readily satisfy both requirements, benefiting from large electronic absorption cross-sections ($\sim 10^{-17}$–10^{-15} cm^2), high quantum yields, and ultra-sensitive, low-noise detectors (capable of single-photon counting), which explains the widespread usage of fluorescence-based techniques in the SM community.

However, conventional vibrational spectroscopies have lagged in sensitivity due to failing in (at least) one of these requirements. IR absorption cross-sections can be sufficiently large (generally $\sim 10^{-19}$–10^{-17} cm^2),[32] but sensitive IR detection is challenging. IR spontaneous emission rates are exceedingly slow (~μs) compared to the competing non-radiative vibrational decay pathways at room temperature (~ps). Therefore, direct absorption is the default detection method in the IR, which suffers from large background noise and fluctuation (unlike detecting fluorescence at a new wavelength, where background from the excitation light source can be filtered out). Furthermore, direct measurement of mid-IR photons requires the use of noisier detectors.[33–35] As a result, IR absorption measurements commonly occur in the mM concentration range,[36] operating quite far from SM sensitivity.

In contrast, spontaneous Raman scattering cross-sections are inherently small (typically $\sim 10^{-30}$–10^{-28} cm^2), but Raman scattering does not require optical sources to be resonant with the excited vibrational transitions. Thus, Raman-based approaches can use the same robust laser and detector technologies as fluorescence-based methods, theoretically having access to much better sensitivities with extensive averaging.[37] In practice, however, spontaneous Raman measurements are also generally limited to high concentrations, since very long exposure times can be complicated by factors like drift and cosmic spikes.

1.1. Far-field and near-field methods

Despite these inherent limitations of IR and Raman methods, clever experimental strategies have granted massive sensitivity improvements (Fig. 1). These strategies can be broadly classified as "far-field" and "near-field" methods (see the Definitions section). Far-field techniques (Fig. 1a) are highly compatible with many different sample types, including bulk samples, liquids, and tissues, and are well-established as being non-perturbative, making them attractive towards general-purpose, sample-agnostic methods. Near-field methods, commonly utilizing nanoscale tips, surfaces, nanoparticles, or tapered fibres (Fig. 1b), achieve remarkable spatial resolution and

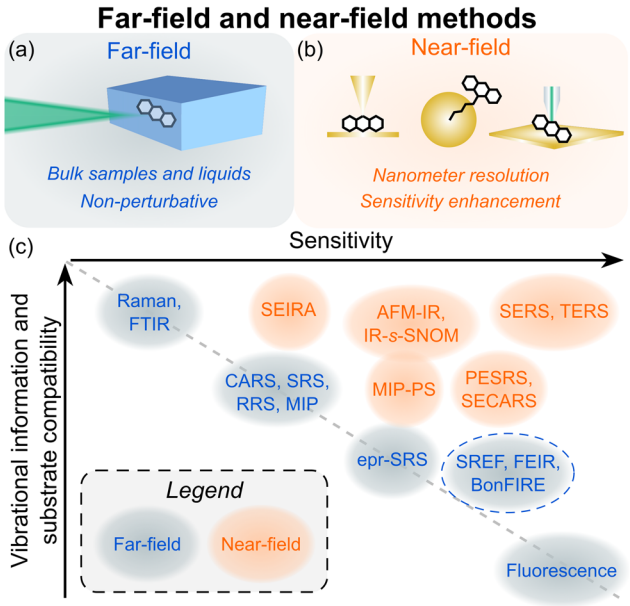

Fig. 1 Summary of far-field and near-field vibrational spectroscopic methods. Schematic depictions of (a) far-field (blue) and (b) near-field (orange) optical methods, each with unique advantages and tradeoffs. (c) Illustrative comparison of vibrational spectro-microscopies as a function of sensitivity (horizontal axis) and a combination of vibrational information and substrate scope (vertical axis). The grey diagonal line illustrates a persistent tradeoff, where gains in sensitivity are generally accompanied by losses in substrate compatibility or spectral information. In this Perspective, we discuss the first far-field methods to have escaped this diagonal (SREF, FEIR, and BonFIRE). Abbreviations are elaborated in the Definitions section.

increased sensitivity. Although near-field methods face challenges with complex spectral lineshapes[38] and possible perturbations of molecular properties,[39] their massive sensitivity enhancements allowed for near-field vibrational spectro-microscopies to break the SM barrier nearly three decades ago. In contrast, far-field vibrational spectro-microscopies have lagged significantly in sensitivity, due to a persistent tradeoff between sensitivity and a combination of vibrational information and applicable substrate scope. We qualitatively illustrate this tradeoff in Fig. 1c (dashed grey diagonal line), summarizing the scope of techniques that we will discuss here.

1.2. Overview and scope

In this Perspective, we will primarily focus on the development of three emerging far-field methods: stimulated Raman-excited fluorescence (SREF), fluorescence-encoded infrared (FEIR), and bond-selective fluorescence-detected infrared-excited (BonFIRE) spectro-microscopies (Fig. 1c, blue-outlined oval). Collectively, these methods are the first vibrational spectro-microscopies to break the SM barrier even with far-field optics, highlighting their importance in modern physical chemistry.[40,41] In Section 2, we present the foundational principles underscoring each of these methods, demonstrating that these complex experimental techniques can be conceptualized from a unifying, global framework. In Section 3, we provide a brief review of far-field SM vibrational spectro-microscopies

(SREF, FEIR, and BonFIRE), summarizing recent work and providing an integrative comparison. In Section 4, we discuss the outlook of these methods toward exciting future applications.

Despite our focus on the far-field methods, we will start by discussing near-field principles and methods, as the landscape of SM vibrational spectroscopy has been largely shaped by these near-field approaches. Thus, we believe that a discussion of current near-field methods is necessary to provide the proper context for understanding where the far-field methods can shine. We argue that this integrative approach will better inform the development, importance, and application spaces for future far-field work.

2. Foundations of SM vibrational spectroscopy

In the framework we established in the Introduction, achieving SM sensitivity in vibrational spectroscopy requires either (1) enhancing the signal intensities or (2) improving detection sensitivity. In this section, we discuss several approaches to addressing these two challenges, showing that they can be conceptualized as discrete "building blocks" that serve as the foundations of SM vibrational spectroscopy and imaging.

2.1. Enhancements to Raman scattering signals

Multiple strategies have been developed to overcome the inherently small cross-sections of spontaneous Raman scattering, which can be broken down into three categories: coherent Raman scattering, resonance Raman scattering, and plasmon-enhanced Raman scattering (Fig. 2).

In coherent Raman scattering (Fig. 2a), a pair of lasers is tuned such that the difference in their frequencies resonates with the vibration of interest.[42–44] The two most widely used forms of coherent Raman scattering are coherent anti-Stokes Raman scattering (CARS) and stimulated Raman scattering (SRS).[45] In particular, SRS has found broad adoption in recent years due to minimal non-resonant background and a straightforward linear concentration dependence, among other practical factors.[46]

The SRS excitation scheme results in an enhancement of up to $\sim 10^6$–10^8-fold compared with spontaneous Raman scattering, benefiting from signal amplification similar to stimulated emission.[24] Recent theoretical work has shown that SRS can be understood from the perspective of Einstein's coefficients, providing new insights into the inherent strength of the SRS process from a quantum mechanical viewpoint.[47,48] The signal enhancement provided by SRS alone is sufficient to allow label-free bioimaging with high detail,[20] fuelling the development of SRS as a workhorse in modern chemical imaging. However, SRS cross-sections ($\sim 10^{-24}$–10^{-22} cm^2) are still far from SM sensitivity, typically achieving detection limits in the 0.1–10 mM range.[25]

Another strategy to improve Raman cross-sections is by using a laser that is tuned (near) to a real electronic transition of the target molecule, termed (pre-)resonance Raman scattering (Fig. 2b). Through vibrational-electronic (vibronic) coupling with a strong electronic resonance, the Raman scattering process can be enhanced by up to $\sim 10^7$-fold ($\sim 10^{-23}$ cm^2),[49] generally yielding detection limits in the 10–100 μM range with deep-ultraviolet excitation.[50]

The third category of Raman signal enhancement leverages localized surface plasmon resonance of metallic nanostructures (Fig. 2c), where the oscillations of the electron cloud on a metal surface create "hot spots" with very intense electric fields (often at the interface between two nanoparticles).[51] These hot spots form the basis of surface-enhanced Raman scattering (SERS) and tip-enhanced Raman scattering (TERS), yielding Raman signal enhancements of $\sim 10^5$–10^{11}-fold due to the strength of the field.[52]

Initially, none of these enhancement mechanisms individually yielded sufficient enhancement to achieve SM Raman spectroscopy. However, by combining two enhancement mechanisms, Raman signals can be sufficiently enhanced for SM detection. For example, by combining plasmonic enhancement with resonance Raman scattering, resonance-enhanced SERS and TERS were the first vibrational spectroscopies to

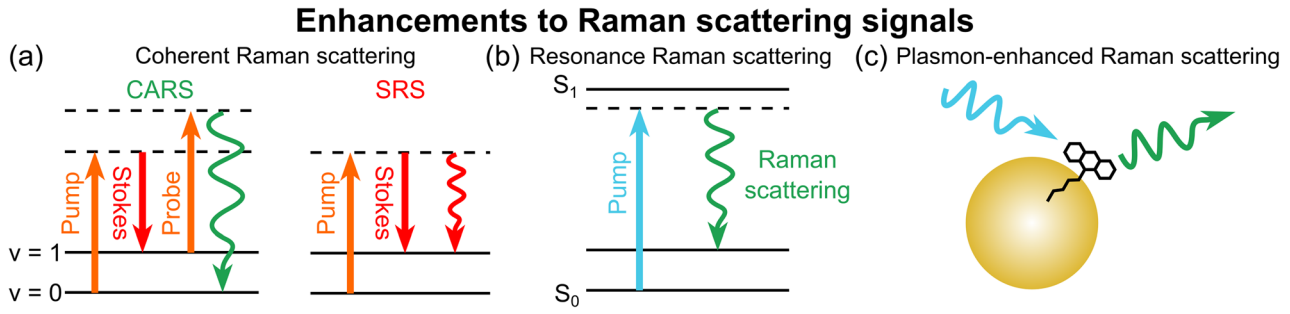

Fig. 2 Raman scattering enhancements. (a) Coherent Raman scattering. A pair of lasers (pump and Stokes) whose difference-frequency is resonant with the vibrational transition can increase Raman scattering cross-sections by up to $\sim 10^6$–10^8-fold. In coherent anti-Stokes Raman scattering (CARS), the pump also serves as a probe beam, generating a new photon of a higher frequency. In stimulated Raman scattering (SRS), no new frequencies are generated, but the intensities of the pump and Stokes beams are modulated through the SRS process. (b) Resonance Raman scattering. Pumping the Raman transition with a laser that is (pre-)resonant with a real electronic transition can increase Raman scattering cross-sections by up to $\sim 10^7$-fold. (c) Plasmon-enhanced Raman scattering. The large electric fields generated at the surface of a metallic nanoparticle or tip can increase Raman scattering signals by $\sim 10^5$–10^{11}-fold.

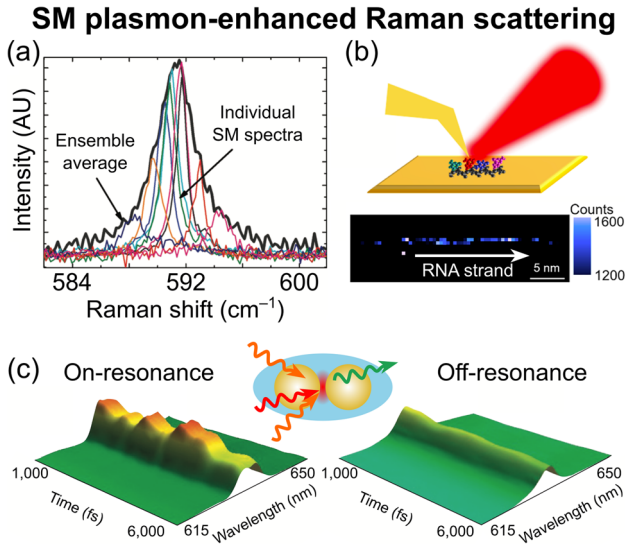

Fig. 3 SM plasmon-enhanced Raman scattering. (a) Example SM-SERS spectra, showing that an inhomogeneously broadened ensemble average can be decomposed into contributions of individual molecules (adapted with permission from ref. 56. Copyright 2010 American Chemical Society). (b) RNA sequencing by SM-TERS. Unique fingerprints can be obtained for each of the four nucleobases (adapted with permission from ref. 57. Copyright 2021 American Chemical Society). (c) SM time-resolved surface-enhanced CARS. Coherent oscillations can be observed from a single molecule held between two Au nanoparticles in a silica shell (adapted with permission from ref. 61. Copyright 2014 Springer Nature).

achieve SM sensitivity.[51,53–55] We here note that SM-SERS with non-resonant probes was later reported for hot spots approaching the theoretical maximum enhancement.[52]

With SM sensitivity, inhomogeneous broadening (reflecting ensemble-averaging of molecules with different center frequencies) is removed, allowing for the direct visualization of individual molecules (Fig. 3a).[56] SM-SERS and SM-TERS have both found application in electrochemical systems, allowing for studies of chemical reaction dynamics and catalysis at the SM level.[51] An interesting application of SM-TERS in the biological sciences is RNA sequencing (where the four nucleobases each have unique Raman fingerprints), which was recently reported (Fig. 3b).[57]

The combination of coherent Raman scattering with plasmonic enhancement for SM detection was first reported in 2005,[58] utilizing surface-enhanced CARS (SECARS).[59] SECARS quickly became a powerful SM method[60] and was later revisited by Potma and co-workers in 2014.[61] With time-resolved SECARS, coherent oscillations on ultrafast timescales were directly visualized at the SM level (Fig. 3c), yielding detailed insights into the noise profiles and statistics of very small molecular ensembles. More recently, Cheng and co-workers demonstrated SM sensitivity by combining SRS with plasmonic enhancement.[62] Overall, the combinations of plasmonic enhancements with other Raman cross-section enhancements have proven quite successful in achieving SM Raman spectroscopy. However, these near-field approaches require the samples to be in the close vicinity of metallic surfaces, which omits the detection of free molecules and suffers from challenging quantification and possible protein denaturation, especially inside biological cells.

For all far-field Raman cross-section enhancements, the combination of SRS and resonance Raman scattering would also theoretically allow for SM sensitivity (theoretical cross-sections on the order of 10^{-16} cm^2), but such measurements are complicated by pump–probe background signals.[49] Detuning from strict resonance to the electronic pre-resonance regime (epr-SRS) provides a balance of signal-to-noise and signal-to-background, allowing for super-multiplex vibrational imaging in live cells.[26] In its initial demonstration, epr-SRS achieved 250 nM sensitivity,[26] corresponding to 30–50 molecules within the focal volume, but despite significant theoretical and experimental efforts towards brighter probes,[63] epr-SRS microscopy has not yet broken the SM barrier.

2.2. Enhancements to IR absorption signals

Several strategies have also been developed to enhance IR absorption spectroscopy (Fig. 4). As with Raman scattering, IR absorption also experiences a signal enhancement for probes held near a plasmonic surface, termed surface-enhanced IR absorption (SEIRA; Fig. 4a, left). However, the signal enhancements in SEIRA are more modest than those in SERS, with typical enhancements on the order of 10^2–10^5-fold.[64–66]

A related approach is IR scattering-type scanning near-field optical microscopy (IR-s-SNOM),[67] where IR light is irradiated on a sample near a metallic tip (enhanced due to confinement), and the scattered light is interferometrically detected (Fig. 4a, right).[66] Raschke and co-workers achieved detection of ~100 molecules with IR-s-SNOM, noting potential for further improvement by inclusion of a resonant antenna and higher-power lasers.[38]

An alternative strategy for improving direct IR absorption sensitivity is the use of an optical cavity (Fig. 4b), which has become a gold standard in the gas phase for ultrasensitive measurements and studies of kinetics and dynamics.[68] By passing a beam of light through a sample many times, the effective optical path length can be massively amplified, routinely allowing for sensitivity improvements on the order of 10^2–10^3 with high-finesse cavities.[69] In the condensed phases, plasmonic microcavities hold particular promise, combining the plasmonic and cavity enhancements for highly sensitive optical detection.[70,71]

New optical pulse sequences can also afford enhanced IR absorption detection, and these enhancements can extend beyond sensitivity improvements. Bredenbeck and co-workers described an example of this concept with their vibrationally promoted electronic resonance (VIPER) technique (Fig. 4c).[72] In this manner, the short vibrational lifetime (~ps) is exchanged for a long electronic lifetime (~ns), allowing for vibrational probing of ultrafast chemical exchange for over 100 ps – well beyond the vibrational lifetime.[72]

While there are notable successes, improvements to IR absorption remain orders of magnitude behind those of Raman scattering in absolute signal enhancement. However, for IR

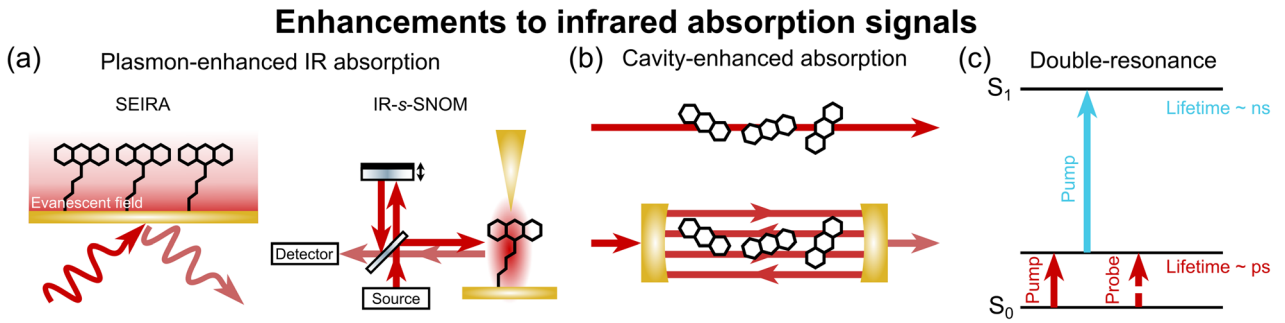

Fig. 4 IR absorption enhancements. (a) Plasmon-enhanced IR absorption. Similar to Raman scattering, IR absorption intensities are amplified by interactions with surface plasmons (surface-enhanced IR absorption; SEIRA), but only by ~10^1–10^3-fold without resonance. IR scattering-type scanning near-field optical microscopy (IR-s-SNOM) also benefits from plasmonic enhancement, with interferometric detection allowing for retrieval of spectral information. (b) Cavity-enhanced absorption. By passing a beam of light through a sample many times, the absorption is increased by ~10^2–10^3-fold. (c) Double-resonance spectroscopy. The short observation window of the IR-excited lifetime (~ps) is extended to the length of the electronic excited state (~ns), allowing for dynamic measurements well beyond the vibrational lifetime.

absorption, as we noted in the Introduction, the cross-sections can already be sufficiently large; the main issue is that the direct detection of IR photons remains challenging, due to large background fluctuations and noisier, small-bandgap detectors. These inherent constraints have motivated significant work towards devising methods for detecting IR absorption indirectly, by inferring through another observable that is easier to measure. These methods are broadly known as action spectroscopies.

2.3. Vibrational action spectroscopy

Action spectroscopies are a class of spectroscopic techniques where a complementary but related observable is used as an indirect measure of absorption. Action spectroscopy is at the core of many modern spectroscopic methods in the gas[73–76] and condensed phases,[77–83] generally affording much improved sensitivity over direct absorption techniques. While absorption techniques are appealing due to their general applicability and SM detection is indeed possible with direct absorption spectroscopy, these methods generally entail significant effort to minimize noise and background, such as cooling to cryogenic temperatures[1] or multiply balanced detection.[84] In contrast, action-detected methods generally offer background signals that are minimal, easily removed, or both, and often they are explicitly sought for high-performance, low-noise detection.

In the condensed phases, several action-detected techniques have been developed towards high-sensitivity vibrational spectroscopy (Fig. 5). Among the earliest SM vibrational action spectro-microscopies is scanning tunnelling microscopy-inelastic electron tunnelling spectroscopy (STM-IETS), as demonstrated by Ho and co-workers (Fig. 5a).[85] In STM-IETS, electrons tunnel inelastically, transferring energy to molecular vibrations and leading to characteristic peaks in the second derivative of the current (at constant height) as a function of the applied voltage.[86] IETS is unique as a SM vibrational technique that requires no light source, providing an interesting perspective for controlling chemistry on surfaces.[87]

The generation of heat following non-radiative relaxation is persistent (and often deleterious) in optical vibrational spectroscopies. However, because heat can lead to many measurable local alterations, such as thermal expansion and thermal lensing, several groups have developed action spectroscopic strategies that focus on detecting the heat released following vibrational excitation (Fig. 5b).

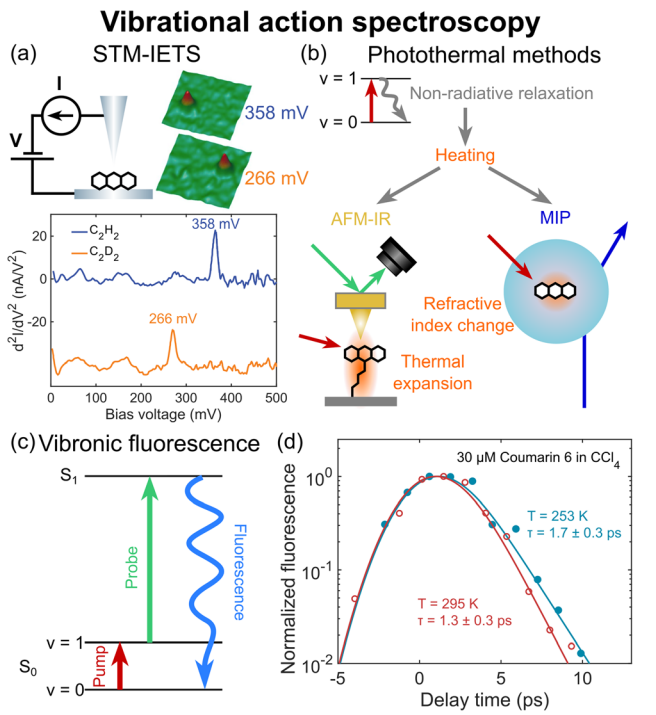

Fig. 5 Vibrational action spectroscopy. (a) Scanning tunnelling microscopy-inelastic electron tunnelling spectroscopy (STM-IETS). Inelastic tunnelling results in electron energy loss to molecular vibrations, allowing for vibrational spectra to be recorded as a function of an applied voltage (from ref. 85. Adapted with permission from AAAS, copyright 1998). (b) Photothermal methods. Several action techniques detect the heat generated following non-radiative vibrational decay. Examples include atomic force microscopy-coupled IR spectroscopy (AFM-IR; left) and mid-IR photothermal spectroscopy (MIP; right). (c) Energy-level diagram for IR-excited vibrational-electronic double-resonance with fluorescence detection. (d) Vibronic fluorescence as a probe of vibrational lifetimes (adapted with permission from ref. 88, copyright Elsevier 1975).

A powerful near-field approach for probing thermal expansion is atomic force microscopy-coupled IR spectroscopy (AFM-IR; Fig. 5b, left), where the deflection of an AFM cantilever is probed following IR-induced thermal expansion.[89] A recent report described AFM-IR at the single-protein level, achieved by intentionally detuning the IR laser repetition rate away from the natural cantilever resonances.[90] In the far field, Cheng and co-workers have pioneered the development of vibrational photothermal bioimaging techniques,[91] beginning from the mid-IR photothermal (MIP) effect (Fig. 5b, right), which have seen significant development and adoption over the past decade.[92–96] Towards improved sensitivity, Cheng and co-workers recently achieved a detection sensitivity of ~130 molecules by combining MIP with plasmonic enhancement.[97]

Naturally, among the most sensitive action spectroscopies are those that employ fluorescence detection.[98–100] For the molecular vibrations of interest, the question then becomes how best to couple vibrational spectroscopic observables to fluorescence. This question is certainly not new, and the first successful report well pre-dates SM spectroscopy. In 1975, Laubereau, Seilmeier, and Kaiser described fluorescence-detected vibronic double-resonance spectroscopy (Fig. 5c).[88] In their method, a fluorescent dye (*e.g.*, Coumarin 6) is first excited by a resonant mid-IR (pump) pulse. A second, visible-frequency (probe) pulse arrives while the molecule is still vibrationally excited, up-converting the molecule to a fluorescently active state. In this scheme, under the assumption that the fluorescence quantum yield is independent of how the molecule reaches the S_1 manifold (which is reasonable under Kasha's rule, given the vastly different timescales of vibrational and electronic relaxation), the total fluorescent signal is directly proportional to the vibrationally excited population.

Kaiser and co-workers used their vibronic fluorescence technique primarily for fundamental studies of ultrafast vibrational dynamics in liquids.[101] Because they used ultrashort (<10 ps) pulses, they could directly measure the lifetimes of excited vibrational states on the picosecond timescale by delaying the arrival time of the visible pulse relative to the mid-IR (Fig. 5d).[88] These experiments provided entirely new understandings of vibrational energy flow in large molecules, and Kaiser and co-workers' body of work reflects their evolving understanding of these dynamics over the 1970s–80s.[102–104] Kaiser and co-workers' pioneering efforts laid the foundation for far-field SM vibrational spectroscopy, and they were keenly aware of the potential of their work for broader applications in chemistry and biology.[105,106]

A handful of other groups also explored such strategies in early pioneering work, towards SM Raman spectroscopy and super-resolution IR microscopy. In 1980, Wright theoretically explored the stimulated Raman-pumped analogue of Kaiser's vibronic fluorescence strategy;[107] later attempts to realize this concept were unsuccessful, with Wright and co-workers noting an overwhelming two-photon fluorescence background that was roughly 20-fold larger than the fluorescence estimated from the Raman-pumping strategy.[108] Orrit and co-workers later revisited this strategy with numerical simulations, finding that it could offer SM sensitivity at room temperature if achieved.[109]

Adopting a similar strategy to Kaiser, Sakai and Fujii described transient fluorescence-detected IR (TFD-IR) spectroscopy.[78] Recognizing that the diffraction-limited focus of the up-conversion probe beam is much tighter than the diffraction-limited IR focus, Sakai, Fujii, and co-workers demonstrated super-resolution IR imaging[110] and noted the potential for further improvement with saturation effects.[111] In more recent work, Sakai and co-workers demonstrated that flavin mononucleotide is compatible with TFD-IR,[112] laying the foundation for TFD-IR imaging with endogenous fluorophores.

In the current era, Mastron and Tokmakoff were the first to revisit Kaiser's vibronic fluorescence spectroscopy, combining strong IR absorption cross-sections and fluorescence-detected action spectroscopy with modern laser instrumentation.[36] In their strategy, which they named fluorescence-encoded IR (FEIR) spectroscopy in 2016, they employed broadband femtosecond pulses generated *via* optical parametric amplification, allowing them to directly measure multimode vibrational coherent oscillations in fluorescent intensity,[36] and they subsequently developed FEIR with Fourier transform detection.[113] In their initial FEIR studies, Mastron and Tokmakoff used a two-photon absorption for the electronic up-conversion, which ultimately limited their sensitivity.[113]

3. Far-field SM vibrational spectroscopy and imaging

Near-field approaches have had strong successes in achieving SM vibrational spectroscopy, allowing for detailed *in situ* profiling applications and holding promise for SM electrochemistry and catalysis.[51] However, all-far-field SM approaches remain highly desirable in modern applications. Lifting the requirement of a metallic tip or nanoparticle means that far-field approaches can be much less perturbative, particularly for measurements on biological molecules. Far-field techniques also maintain excellent compatibility with samples such as thick biological tissues and bulk liquids. Furthermore, the complications resulting from near-field polarization and tip-sample couplings often give rise to complex lineshapes, making spectral interpretation challenging.[38] Additionally, given that near-field SM vibrational methods have already been extensively reviewed elsewhere,[51,87,114] we limit our focus to far-field approaches for achieving SM vibrational spectroscopy under ambient conditions for the remainder of this Perspective.

3.1. Stimulated Raman-excited fluorescence spectroscopy and imaging

It was known well in advance that the ultimate sensitivity of fluorescence detection was a promising avenue for achieving far-field SM vibrational spectroscopy,[88] but it took nearly 50 years to be realized experimentally. The first all-far-field SM vibrational spectroscopy and imaging technique was stimulated Raman-excited fluorescence (SREF), as reported by Min and co-workers in 2019 (Fig. 6).[115] Conceptually, SREF is a fluorescence-detected action spectroscopy based on epr-SRS-vibrational excitation (Fig. 6a). As anticipated from early studies,[107,109]

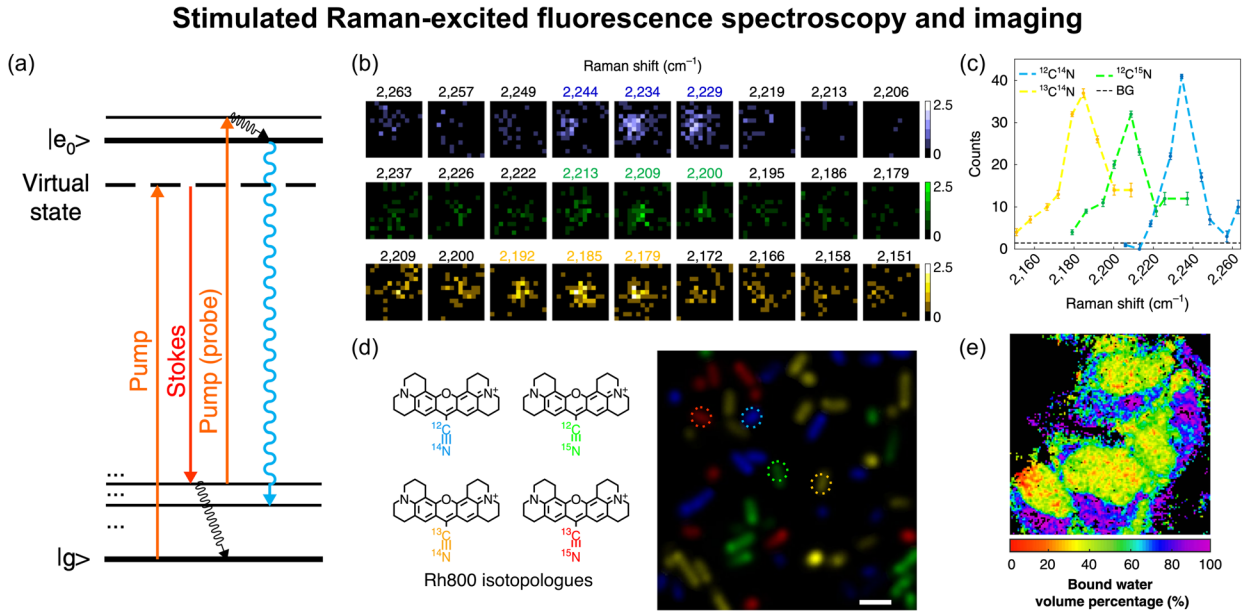

Fig. 6 SREF spectroscopy and imaging. (a) Principle of SREF, comprising an epr-SRS vibrational excitation and electronic up-conversion for fluorescence detection (reprinted with permission from ref. 115, copyright 2019 Springer Nature). (b) SREF SM imaging on three nitrile isotopologues. Colour bars are counts per ms (adapted with permission from ref. 115, copyright 2019 Springer Nature). (c) SREF spectroscopy on SMs (reprinted with permission from ref. 115, copyright 2019 Springer Nature). (d) 4-Colour SREF microscopy of live *E. coli*. The Rh800 isotopologues are distinguished by their vibrational frequencies (scale bar: 2 μm) (reprinted with permission from ref. 115, Copyright 2019 Springer Nature). (e) SREF water mapping in live HeLa cells. Bound water content is assessed by the nitrile frequency of Rh800 (reprinted with permission from ref. 117, copyright 2019 Springer Nature).

leveraging fluorescence detection yields a marked sensitivity improvement (~10^3–10^5-fold), but the successful implementation of SREF required the signal enhancement of epr-SRS (and therefore, epr-SRS-compatible dyes) to not be overwhelmed by background fluorescence.[116] Background fluorescence (from the thermal population in vibrationally excited states) remains observable in SREF, but the mode-specific signal of interest can be isolated by sweeping the laser frequency (Fig. 6b and c).[115]

In their initial report, Min and co-workers demonstrated a limit of detection of ~10 nM in solution, ultimately confirming their SM sensitivity by imaging isolated single molecules that were spin-cast into a polymer film from a highly dilute solution (Fig. 6b).[115] They demonstrated SM imaging of three isotopologues of a common near-IR dye, Rhodamine 800 (Rh800), where the isotopologues exhibited identical electronic absorption and emission spectra but were vibrationally distinct (Fig. 6c).[115] Four-colour SREF microscopy on live *E. coli* was further demonstrated, readily differentiating the four major nitrile isotopologues on the basis of their unique vibrational frequencies (Fig. 6d).

Shortly after their initial report, Min and co-workers demonstrated that SREF can report local chemical information, using the nitrile-stretching frequency of Rh800 as a probe of local hydration in live HeLa cells (revealing higher bound water content in the cytoplasm than the nucleus; Fig. 6e)[117] and electric fields at oil-water interfaces.[118] In 2021, Min and co-workers described super-resolution SREF microscopy, achieved by coupling SREF with stimulated emission depletion (STED) and frequency modulation, demonstrating a spatial resolution of ~180 nm (~2-fold below the diffraction limit).[119] Most recently, H. Xiong and co-workers reported transient SREF, achieving 40 nM sensitivity with Fourier transform detection.[120] New developments in SREF should continue to advance both super-multiplex imaging and local environment sensing in vibrational spectro-microscopy.

3.2. Fluorescence-encoded infrared spectroscopy

On the IR side, Tokmakoff and co-workers continued improving on their FEIR method (Fig. 7), implementing FEIR spectroscopy with a one-photon electronic up-conversion in 2019 (Fig. 7a) and achieving Fourier transform spectroscopy in much more dilute solutions.[121] Then, in 2021, by coupling FEIR with fluorescence correlation spectroscopy, Tokmakoff and co-workers achieved SM vibrational spectroscopy with FEIR correlation spectroscopy.[122]

Analogous to Kaiser and co-workers' experiments (Fig. 5d), Tokmakoff and co-workers observe the clear decay of a real vibrational state as the visible "encoding" pulse arrives later than the mid-IR pulses, even at a Coumarin 6 concentration of 1 nM (Fig. 7b).[122] Distinct from SREF's imaging of isolated SMs in polymer films, FEIR's SM sensitivity is evidenced by the fluctuations of fluorescent signals on the microsecond timescale (*i.e.*, fluctuation correlation spectroscopy; Fig. 7c), confirming the SM concentration of 1 nM in FEIR.[122] Utilizing Fourier transform detection, the strong ring-breathing mode of Coumarin 6 (~1586 cm^{-1}) is clearly visible in even a 1 nM solution with 30 min of acquisition time (Fig. 7d), confirming

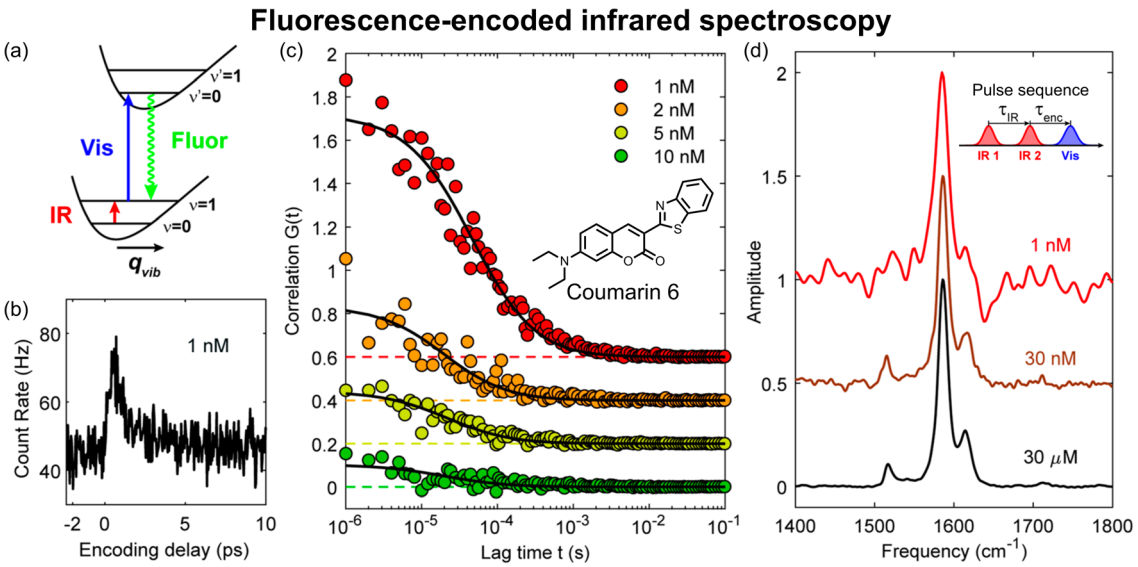

Fig. 7 FEIR correlation spectroscopy at the SM level. (a) Principle of FEIR spectroscopy, comprising linear absorptions with broadband pulses. (b) FEIR signal of Coumarin 6 at 1 nM as a function of the encoding delay (time between the IR and visible pulses). 1 nM is the effective SM concentration. (c) FEIR correlation functions for Coumarin 6 (structure inset) at varying concentrations. (d) FEIR spectra of Coumarin 6 at varying concentrations (pulse sequence inset) (figure panels adapted with permission from ref. 122. Copyright 2021 American Chemical Society).

FEIR's ability to measure vibrational spectra with SM sensitivity.[122]

In more recent work, Tokmakoff and co-workers have contributed substantially (both in experiments and theory) to our fundamental understanding of vibronic fluorescence as a physical process.[123–126] Toward future applications, FEIR spectroscopy holds significant potential for studying solution-phase reaction dynamics, where vibrational frequency shifts upon bond formation or breaking could be used to directly track chemical reactions at the SM level. Such developments in FEIR should be transformative toward broader applications in the chemical sciences.

3.3. Bond-selective fluorescence-detected infrared-excited spectro-microscopy

As with any experimental method, SREF and FEIR each have inherent advantages and limitations. SREF achieves impressive brightness (~2.5 counts per ms at the SM level; Fig. 6b) and biocompatibility, due to its narrowband (2-ps) pulses efficiently exciting narrow-linewidth vibrational modes and high repetition rate (80 MHz), but it requires careful selection of the epr-SRS excitation region (and therefore, epr-SRS-compatible dyes) to not be overwhelmed by background.[115] In contrast, broadband (200-fs) FEIR achieves lower count rates (~0.03 counts per ms, primarily due to the 1 MHz repetition rate; Fig. 7b), but it is more broadly compatible, as it benefits from inherently larger IR absorption cross-sections (from a large reservoir of molecules) rather than being restricted to the pre-resonance Raman regime. We reasoned that a new method, combining narrowband pulses with direct mid-IR excitation, could potentially combine advantages of both SREF and FEIR, with motivations toward achieving wide-field functional SM vibrational imaging in live cells.

In 2023, we reported bond-selective fluorescence-detected IR-excited (BonFIRE) spectro-microscopy (Fig. 8).[127] We employ two narrowband (2-ps) pulses, with the first pulse selectively exciting a mid-IR vibrational mode (Fig. 8a). By scanning our mid-IR laser frequency and measuring relative fluorescent intensity, we can image IR absorption at the SM level, with a limit of detection of 0.5 nM in solution and brightness comparable to SREF at the SM level (~2.5 counts per ms; 80 MHz repetition rate) in the molecular fingerprint region.[127] We reported 3-colour nitrile SM imaging on dyes structurally similar to Rh800, demonstrating the first IR-based multiplex imaging at the SM level (Fig. 8b). Shortly thereafter, we demonstrated that nitrile vibrational lifetimes can serve as probes of local electric fields (Fig. 8c), which we rationalized through identifying the electric field-dependence of the anharmonic couplings governing intramolecular vibrational energy redistribution.[128] Most recently, we described two-dimensional BonFIRE (2D-BonFIRE), leveraging 2D spectral information to achieve 16-colour imaging in the cell-silent region in a proof-of-concept demonstration with drop-cast polystyrene films (Fig. 8d).[129]

A key feature of BonFIRE and FEIR is that IR-excited double-resonance comprises two linear absorptions (rather than the nonlinear Raman excitation in SREF). Therefore, we reasoned that BonFIRE could be adapted to a wide-field (WF) imaging configuration (where the photon fluxes are much lower and spread out over a large area), potentially allowing for real-time imaging.

In recent work, we described WF-BonFIRE, achieving up to kHz imaging speeds and demonstrating video-rate imaging on samples ranging from isolated SMs to live cells and neurons (Fig. 8e).[130] By developing a chopper-based temporal delay modulation scheme, we demonstrated real-time two-colour WF-

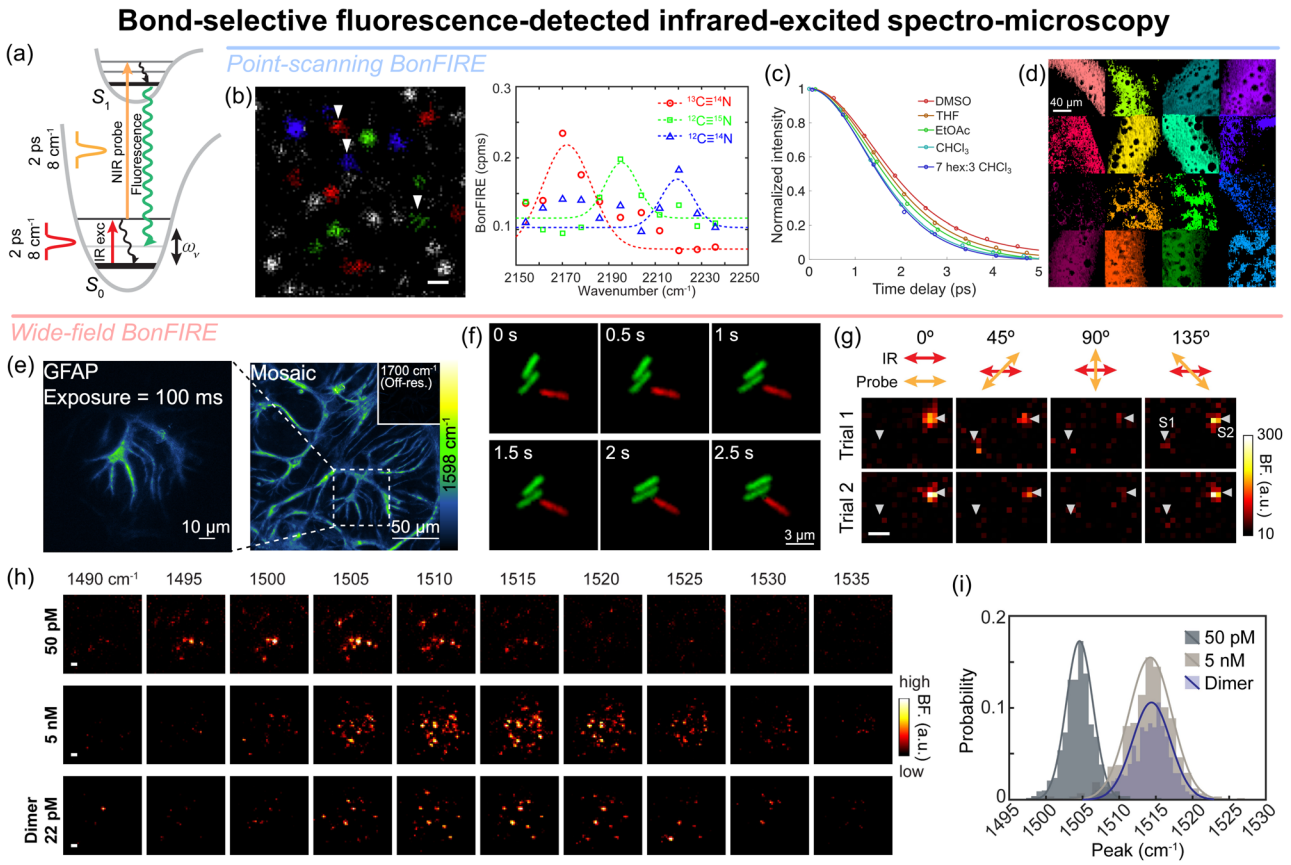

Fig. 8 BonFIRE spectroscopy and imaging. (a) Principle of BonFIRE, comprising two narrowband excitations (adapted with permission from ref. 127, copyright 2023 Springer Nature). (b) 3-colour BonFIRE SM imaging. Three nitrile isotopologues of a dye are distinguished by their nitrile IR frequencies (scale bar: 1 μm) (adapted from ref. 127, copyright 2023 Springer Nature). (c) Local electric field sensing with nitrile vibrational lifetimes, probed by BonFIRE (adapted with permission from ref. 128. Copyright 2024 American Chemical Society). (d) 16-Colour imaging by 2D-BonFIRE. The individual panels are individually labelled polystyrene films with 16 nitrile dyes (adapted from ref. 129 with permission from the Royal Society of Chemistry). (e) Wide-field BonFIRE imaging on immunolabelled GFAP in mouse neuronal co-cultures (reprinted with permission from ref. 130 © Optica Publishing Group). (f) Real-time wide-field BonFIRE imaging of *E. coli* at 150 fps stained with Cy5.5 (green) and Rh800 (red) (adapted with permission from ref. 130 © Optica Publishing Group). (g) BonFIRE polarization anisotropy as a probe of SM molecular orientation (scale bar: 1 μm). Molecule S2 is aligned with the IR polarization and exhibits BonFIRE, but molecule S1 is perpendicular, exhibiting no BonFIRE signal (reprinted with permission from ref. 131, copyright 2024 Wiley-VCH GmbH). (h) Wide-field BonFIRE SM imaging on spin-cast films from 50 pM ATTO680, 5 nM ATTO680, and a synthetic dimer of ATTO680 at 22 pM (scale bars: 1 μm) (reprinted with permission from ref. 131, copyright 2024 Wiley-VCH GmbH). (i) Vibrational frequency distributions from wide-field BonFIRE images on ATTO680 samples. Despite its low concentration, the 5 nM solution appears to form dimers when spin-cast (reprinted with permission from ref. 131, copyright 2024 Wiley-VCH GmbH).

BonFIRE imaging on stained *E. coli* at 150 fps (Fig. 8f). Furthermore, leveraging the polarization sensitivity of BonFIRE (where each absorption cross-section is maximized when the transition dipole vector is aligned with the optical electric field), we demonstrated that WF-BonFIRE polarization anisotropy on immobilized single molecules allows for direct visualization of molecular orientations (Fig. 8g).

We additionally showed that WF-BonFIRE can be used as a probe of local chemical information.[131] By imaging spin-cast thin films with ATTO680 (another common near-IR dye) prepared at different concentrations, we observed a surprising frequency shift of ~10 cm^{-1} in highly dilute films (50 pM) relative to higher-concentration films (5 nM) and bulk measurements (Fig. 8h).[131] Suspecting that molecular aggregation may be involved, we prepared a synthetic dimer of ATTO680 *via* click chemistry and imaged the dimer under similar conditions (22 pM; Fig. 8h), finding that the dimer frequencies overlapped with the higher-concentration monomer measurements (Fig. 8i).[131] Coupled with density functional theory, our data suggested that ATTO680 dimers could be observed even in samples that appear as isolated SMs under a fluorescence microscope.

To facilitate a comparison between SREF, FEIR, and BonFIRE, we summarize the demonstrated spectroscopy and imaging parameters and performance of each of these methods in Table 1. However, we caution that such a comparison is highly nontrivial, as imaging parameters and performance are strongly sample-dependent and tied to the signal-to-noise ratio. Without a standard sample measured with all three methods, it is challenging to definitively compare imaging performance. Moreover, these methods are all areas of active research, and we expect that continued technical developments will soon surpass

Table 1 Comparison of demonstrated spectroscopy and imaging performance of SREF, FEIR, and BonFIRE

Method	SREF[115]	FEIR[122]	BonFIRE[127]
Vibrational excitation	epr-SRS (mode-selective)	IR absorption (multimode)	IR absorption (mode-selective)
Detection	Fluorescence up-conversion	Fluorescence up-conversion	Fluorescence up-conversion
Working conditions	$\omega_{pump} - \omega_{Stokes} = \omega_{vib}$ $2\omega_{pump} - \omega_{Stokes} \approx \omega_{abs}$ $\omega_{abs} - \omega_{pump} \in (1400, 4200)$ cm^{-1}	$\omega_{IR} = \omega_{vib}$ $\omega_{IR} + \omega_{vis} \approx \omega_{abs}$	$\omega_{IR} = \omega_{vib}$ $\omega_{IR} + \omega_{probe} \approx \omega_{abs}$
Spectral measurement	Narrowband, laser-scanning	Broadband, interferometric	Narrowband, laser-scanning
Spectral resolution	~10 cm^{-1}	~1.3 cm^{-1} (ref. 121)	~10 cm^{-1}
Minimum resolvable vibrational lifetime	N/A	~40 fs	~200 fs (ref. 128)
Repetition rate	80 MHz	1 MHz	80 MHz
Imaging modalities	Point-scanning	Point-scanning[121]	Point-scanning and wide-field
Spatial resolution	~400 nm (diffraction-limited) ~180 nm (super-resolution)[119]	~430 nm (diffraction-limited)[121]	~400 nm (diffraction-limited)[130]
Temporal resolution (imaging)	2 ms pixel dwell time	30 min pixel dwell time (whole IR spectrum)	1 ms pixel dwell time (point-scanning)[129] 20 ms exposure (wide-field, 12.5 μm × 12.5 μm)[130]
SM brightness	~2.5 counts per ms	~0.03 counts per ms	~2.5 counts per ms
Biological compatibility	*E. coli*, HeLa,[117] Cos7,[119] *S. cerevisiae*[119]	N/A	*E. coli*,[130] HeLa, mouse neuronal co-cultures and brain tissue slices
Single-shot multiplexing	4 colours	N/A	16 colours[129]
Local environment sensing	Vibrational frequency[117]	N/A	Vibrational frequency[131] and vibrational lifetime[128]

the demonstrated performance tabulated here, especially given the rapid growth of the field in the last few years.

Leveraging mid-IR absorption grants broader compatibility but also means that BonFIRE and FEIR both must contend with photothermal heating from solvent mid-IR absorption (particularly in the molecular fingerprint region).[92] However, we are optimistic about continuing to develop technical solutions to address these issues, such as the high-frequency modulation[127,128] or temporal delay modulation[130] methods we have described previously that enabled photothermal-free BonFIRE imaging. In the coming years, we will continue developing BonFIRE as a tool for fundamental spectroscopy, chemical imaging, and biological investigations.

3.4. Emerging methods

Within the past few years, multiple groups have independently adopted similar strategies to achieve sensitive vibrational spectro-microscopy. W. Xiong and co-workers described multidimensional widefield IR-encoded spontaneous emission (MD-WISE) microscopy,[132] demonstrating multiplex imaging of fluorescent dyes and quantum dots by leveraging the ability of IR pulses to disrupt excitons. Zheng and co-workers have described a handful of experiments with mixed ps and fs pulses and resolution of the emitted fluorescence,[133–135] demonstrating that these vibronic fluorescence techniques can alternatively be viewed as mode-selective control of electronic properties. Most recently, Yi and co-workers described a single experimental apparatus capable of detecting IR-excited vibronic fluorescence and Raman scattering, demonstrating detection of ~100 molecules using plasmonic nanocavities prepared from silver microspheres deposited on gold film.[136] In 2023, Baumberg and co-workers demonstrated that such a nanocavity-based approach is capable of SM vibrational spectroscopy.[82]

Novel combinations of the various signal enhancement mechanisms described in Section 2 hold significant promise for achieving general-purpose, broadly useful SM vibrational spectro-microscopy without relying on fluorescence detection. For example, we recall that epr-SRS achieved a limit of detection corresponding to 30–50 molecules.[26] Noting that SRS with photothermal detection recently reported over an order of magnitude improvement in sensitivity compared with SRS,[93] we speculate that photothermal-detected epr-SRS may allow for fluorescence-free SM vibrational spectroscopy in the far field, opening up new possibilities for future experiments.

4. Potential applications

Within the past decade, SM vibrational imaging has been achieved without plasmonic enhancement by merging vibrational spectroscopy with fluorescence detection.[40] However, the signals in such experiments are still weaker than their purely fluorescence-based counterparts.[122] Thus, we expect that the most meaningful SM vibrational spectroscopy and imaging experiments will be those that provide information or capabilities inaccessible to conventional fluorescence-based methods, thereby justifying the additional experimental complexity associated with current far-field SM vibrational methods.

As we established in the Introduction, three of the established advantages of vibrational spectroscopy are (1) small, non-perturbative tags, (2) intrinsically narrow linewidths to facilitate super-multiplex imaging, and (3) local environment sensing with physical interpretability. A major shortcoming of the

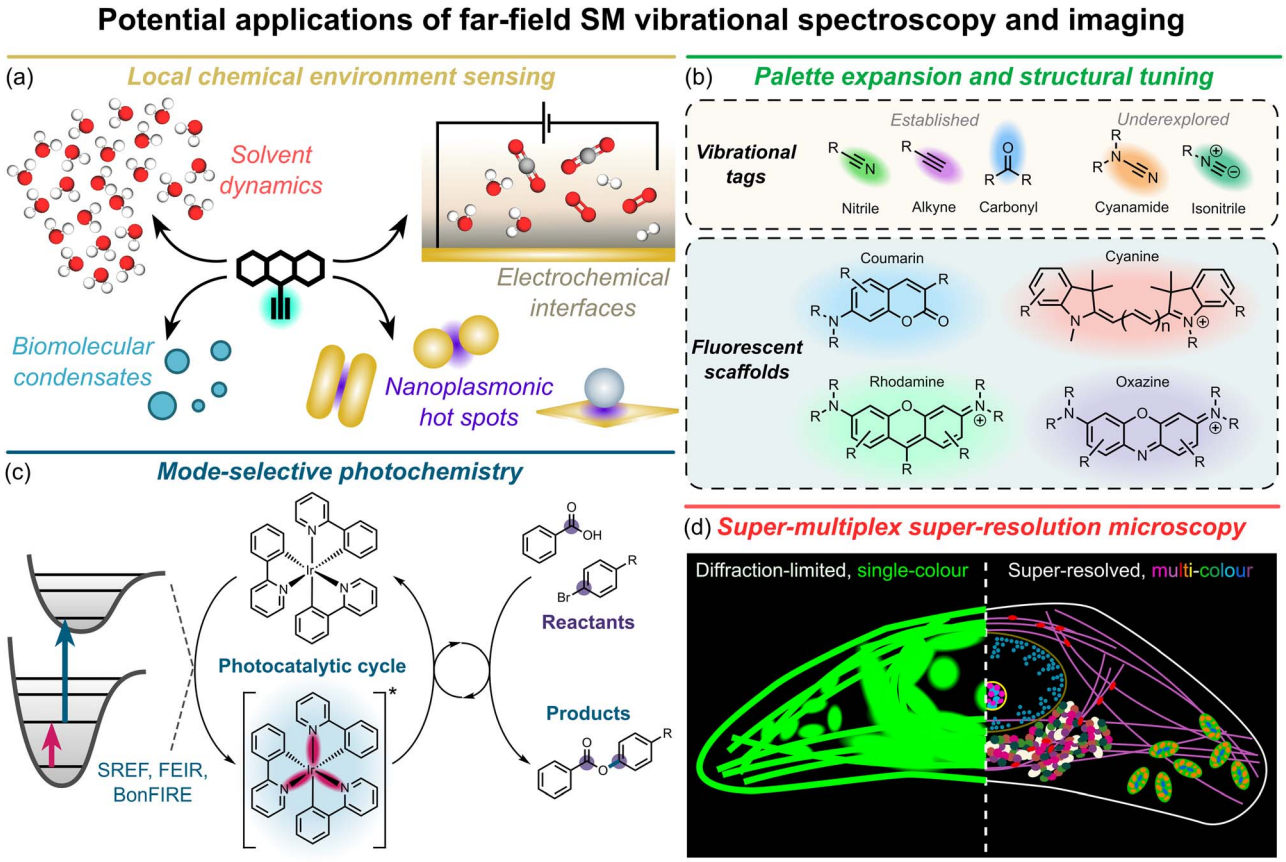

Fig. 9 Potential applications of far-field SM vibrational spectroscopy and imaging. (a) Using SMs as reporters of local chemical information. (b) Expanding the palette of vibrational tags and elucidating structural influences on physical properties. (c) Mode-selective photochemistry at the SM level. (d) Super-multiplex vibrational super-resolution microscopy.

fluorescence-detected SM vibrational spectroscopies reviewed here is the requirement of a fluorophore; hence, the first advantage is effectively traded for SM sensitivity. Thus, in our view, future efforts in these SM vibrational methods should focus on realizing the other two unique functional advantages of vibrational spectroscopy (super-multiplex imaging and quantitative local environment sensing) in real chemical and biological systems. With an eye toward the next decade of SM vibrational spectroscopy and imaging, we outline a few examples of such experiments here (Fig. 9).

4.1. Using SMs as reporters of local chemical information

Obtaining local chemical information at the SM level is a well-established goal of SM spectroscopy and remains a persistent challenge. For example, in the field of fluorescence thermometry, confounding local environment effects are a ubiquitous limitation in obtaining unambiguous quantitative temperatures.[137] In contrast, methods based on vibrational structure have significant potential in quantitative thermometry,[138] and we recently demonstrated one such method (based on excitation in the Boltzmann edge) with SM sensitivity.[139] Thus, SM vibrational methods have the potential to offer unambiguous quantitation in local sensing (Fig. 9a).

Indeed, both SREF and BonFIRE have already made strides in this direction, including probing hydration and local electric fields.[117,118,127,128] Translating these bulk measurements to the SM level may face multiple challenges, but our recent work with BonFIRE and vibrational thermometry indicates that it is feasible to probe chemical information at the SM level with current instrumentation.[131,139]

As with SM fluorescence spectroscopy, the power of a SM vibrational local probe likely lies in its ability to reveal sub-ensemble heterogeneity or dynamics.[6] For example, with fast enough acquisition (and possibly facilitated by lower temperatures), a SM vibrational electric field probe could directly resolve transient solvent behaviours, such as hydrogen-bond fluctuations, solvent reorganization, and solvent tumbling, where the changes in the alignment of solvent dipoles relative to the solute could lead to different local electric fields (Fig. 9a, top left).[128] Probing such behaviours in bulk liquids would be interesting in its own right, but these experiments could provide a fascinating view of enzyme catalysis, where electric fields provide a valuable, quantitative framework for understanding activity.[140]

In a similar line of thinking, one could imagine a SM vibrational probe diffusing through a complex biological environment, like a multiphase biomolecular condensate (Fig. 9a, bottom left),[141] and allowing for quantitative characterization of the composition of each of the phases, as well as providing the potential to study maturation of the condensate over time.[142]

We also note that SM vibrational reporters could be highly valuable outside of biological contexts. For example, vibrational Stark probes were recently employed in studying electrochemical CO_2 reduction, revealing a correlation between a pH gradient at the electrochemical interface and the onset of CO_2 reduction.[143] In such a context, a vibrational spectroscopic pH probe[28] with SM sensitivity could allow for mapping the spatial heterogeneity at the interface, allowing such gradients to be directly imaged (and potentially tracked dynamically, through the progress of the reaction; Fig. 9a, top right).

Additionally, a SM vibrational reporter of local electric fields could be used to better understand the nature of plasmonic hot spots.[81,82] Given that non-resonant SM-SERS requires plasmonic enhancement to see signal, a complementary, far-field SM probe that is not reliant on plasmonic enhancement could allow for direct, *in situ* characterization of the generated fields at metallic surfaces (both with and without optical activation) that are responsible for the SM sensitivity of SERS and TERS (Fig. 9a, bottom right). Such experiments could also allow for direct investigations of the heterogeneities and dynamics of these fields, providing additional insights to complement the industry-standard electric field simulations that are generally employed.[51] It is our view that near-field and far-field methods need not be mutually exclusive, but they can instead be complementary, as each supplements the shortcomings of the other.

4.2. Expanding the palette of vibrational tags and elucidating structural influences on physical properties

Common to SREF, FEIR, and BonFIRE is the requirement of a molecular fluorophore. However, by the same token, SREF, FEIR, and BonFIRE can provide highly detailed characterizations of the chemical physics and dynamics of molecular vibrations in fluorescent dyes.[128] The sensitivity of these techniques allows for a broader substrate scope, since solubility at high concentrations is no longer a requirement for obtaining high-quality vibrational spectra.

Many open and fundamental questions lie at the interface between these SM vibrational spectroscopies and synthetic chemistry. For example, what new vibrational tags can be compatible with SREF, FEIR, and BonFIRE? Thus far, nitriles, alkynes, and carbonyls have been demonstrated as usable vibrational reporters (Fig. 9b, top).[123,127,144] While azides ($-N_3$) are unlikely to be successful tags for these methods due to their strong fluorescence quenching,[145] cyanamides ($-N-C\equiv N$),[146] isonitriles ($-N\equiv C$),[147] and other novel vibrational tags may further expand the probe palette available to these techniques.

The fluorescent scaffolds used in SREF, FEIR, and BonFIRE also present unique opportunities for tuning vibrational and electronic properties through chemical functionalization (Fig. 9b, bottom). Previous work has shown that scaffold functionalization can broadly tune infrared frequencies[148,149] and even allow very fine ($\sim$1 cm^{-1}) control of nitrile frequencies for epr-SRS.[27] As such, exploring substituent effects in SREF, FEIR, and BonFIRE is likely to be a promising avenue in developing brighter probes. Additionally, such work could provide new fundamental insights into how to tune other physical properties, such as vibrational lifetimes,[128] which remain less explored.[149]

Elucidating structure–spectrum relationships can also serve to advance methods beyond SREF, FEIR, and BonFIRE. For example, future probe design efforts in epr-SRS would also benefit from a deeper understanding of how to tune physical properties through structural modifications.[63] Brighter epr-SRS probes may even provide a path toward non-fluorescence-based SM vibrational spectroscopy in the far field.

4.3. Mode-selective chemistry at the SM level

The question of vibrational mode-selective chemistry has fascinated chemists for many years.[104,150] This field has recently seen a resurgence with strong light-matter coupling in optical cavities (*i.e.*, polaritons),[151–153] towards optical control of chemical reactions. Without the vibrational strong coupling provided by an external cavity, excited-state vibrational lifetimes in the condensed phases ($\sim$ps) are generally much too short to be meaningful drivers of chemical reactions. However, vibrational-electronic double-resonance provides an alternative strategy to achieve vibrational mode-selective chemistry (Fig. 9c).

This concept was described by Bredenbeck and co-workers in 2014, in the initial report of their VIPER method.[72] With VIPER, the vibrationally-selected excited state is prolonged to an effective lifetime on the order of nanoseconds (Fig. 3c), meaning that productive chemistry can occur before the excited state decays. In recent work, Bredenbeck and co-workers extended this principle to sub-ensemble photochemistry, demonstrating isotope-selective photochemical uncaging with VIPER.[154] Though Bredenbeck and co-workers' methods employ IR absorption-based detection at higher concentrations, the underlying ideas should be extensible to SM photochemistry *via* SREF, FEIR, or BonFIRE. We speculate that vibrational-electronic double-resonance excitation of a photocatalyst[155] (toward SM photocatalysis) appears particularly promising as a means of achieving general-purpose, mode-selective chemistry in the liquid phase (Fig. 9c).[156]

4.4. Super-multiplex vibrational SMLM

There are many applications where single-shot profiling of many targets is valuable, from high-throughput permeability screening to many-target biosensing, but a particularly interesting example lies in super-multiplex super-resolution imaging. SREF has already demonstrated super-resolution vibrational imaging in a STED-based configuration.[119] However, as we noted in the Introduction, the highest-resolution optical microscopies are generally SMLMs, which can provide single-nm or even sub-nm spatial resolution,[18,19] potentially providing even greater biological insights. With SM sensitivity and wide-field imaging capabilities (Table 1),[130] SM vibrational imaging approaches should theoretically be amenable to SMLM (Fig. 9d).

Achieving super-multiplex imaging has been a long-standing challenge in SMLM, where the broad emission profiles of conventional fluorophores generally limit multiplexing to 2–5 colours. Very recently, DNA-based point accumulation for imaging

in nanoscale tomography was extended to higher levels of multiplexing (similar methodologies reported in the same issue of Cell by Bewersdorf and co-workers[157] and Jungmann and co-workers[158]), allowing for highly detailed interactomics and spatial proteomics.[157,158] Multiplex SMLM methods generally require fixed biological samples, employing multiple rounds of washing, labelling, and imaging (where even kinetically optimized strategies are limited in speed by diffusion).[157] In such a setting, a vibrational SMLM method that is capable of super-multiplex imaging in a single shot could be transformative, potentially allowing SMLM in live cells. Such an experiment could allow for dynamic interactomics or spatial proteomics, visualizing cell-scale proteome changes with nm-resolution and creating an entirely new paradigm of dynamic SMLM.

There is also significant potential for SREF, FEIR, and BonFIRE to expand the capabilities of existing SMLM approaches. For example, using BonFIRE for a vibrational mode-selective photoactivation could facilitate super-multiplex imaging with photoactivatable localization microscopy (PALM). One appealing feature of this approach is that BonFIRE only needs to provide mode-selectivity; the image acquisition (and therefore expected quality) should then ideally be comparable to PALM. We also believe that other modern optical strategies, such as structured illumination microscopy[159] and spectro-microscopy with quantum light sources,[160] as well as non-optical strategies like background removal with machine learning,[161] are worth exploring towards improved resolution and sensitivity.

5. Conclusion

Far-field SM vibrational spectro-microscopy is still a nascent field, with the far-field SM barrier only being broken within the past decade.[115,122,127] Coupling vibrational spectroscopic observables to fluorescence detection has proven useful, allowing for far-field SM vibrational studies to be carried out under ambient conditions.[131] As these technologies continue to develop and mature, we expect they will find growing applications toward both fundamental and applied chemistry in the coming years.

6. Definitions

Far field: systems where the sample is far from the electromagnetic source, detector, or other electromagnetic enhancement, governed by Fraunhofer diffraction.

Near field: systems where the sample is near the electromagnetic source, detector, or other electromagnetic enhancement, governed by Fresnel diffraction.

Infrared (IR) absorption spectroscopy: measurement of attenuation of IR light by a sample, generally resulting from electric dipole-allowed vibrational transitions.

Raman scattering spectroscopy: measurement of inelastic scattering of light by a sample, generally resulting from electric polarizability-allowed vibrational transitions.

Coherent Raman spectroscopy: use of two (or more) coherent laser fields to more efficiently drive Raman scattering processes, resulting in a Raman signal field that is both enhanced and coherent.

Stimulated Raman scattering (SRS): use of two lasers (pump and Stokes) to drive coherent Raman scattering whose difference-frequency is tuned to match the molecular vibration of interest.

Coherent anti-Stokes Raman scattering (CARS): use of two lasers (pump and Stokes) to drive coherent Raman scattering, detected as signal that is anti-Stokes-shifted from the pump laser.

Resonance Raman scattering (RRS): measurement of Raman scattering with a light source that is resonant with the electronic absorption of the molecule of interest.

Electronic pre-resonance stimulated Raman scattering (epr-SRS): use of SRS with the pump beam tuned to the electronic pre-resonance regime.

Plasmonic enhancement: signal enhancement in vibrational spectroscopies obtained by placing the molecule of interest on a metal nanoparticle, tip, or surface.

Plasmon-enhanced stimulated Raman scattering (PESRS): combination of plasmonic enhancement with SRS.

Cavity enhancement: enhancement of optical path length by placing the molecule of interest inside of an optical cavity.

Double resonance: use of two light sources to sequentially excite two transitions.

Action spectroscopy: absorption spectroscopy carried out by measuring a different observable as an inferred measure of relative absorption (generally affording improved sensitivity).

Mid-infrared photothermal (MIP): detection of mid-IR absorption through differential scattering following thermal lensing and expansion.

Mid-infrared photothermal plasmonic scattering (MIP-PS): combination of MIP and plasmonic enhancement.

Up-conversion: electronic excitation from a vibrationally excited state.

Stimulated Raman-excited fluorescence (SREF): combination of epr-SRS vibrational excitation (mode-selective), electronic up-conversion, and fluorescence action detection.

Fluorescence-encoded infrared (FEIR): combination of mid-IR vibrational excitation (multimode), electronic up-conversion, and fluorescence action detection.

Bond-selective fluorescence-detected infrared-excited (BonFIRE): combination of mid-IR vibrational excitation (mode-selective), electronic up-conversion, and fluorescence action detection.

Author contributions

Conceptualization: P. A. K. and L. W. (equal); H. W. and D. L. (supporting). Writing – original draft: P. A. K. (lead); H. W., R. E. L., D. L., N. N., W. M., and L. W. (supporting). Writing – review & editing: all authors. Funding acquisition, project administration, resources, and supervision: L. W.

Conflicts of interest

There are no conflicts to declare.

Data availability

No primary research results, software, or code have been included, and no new data were generated or analysed as part of this review.

Acknowledgements

P. A. K. is grateful for financial support from a National Science Foundation (NSF) Graduate Research Fellowship (DGE-1745301) and a Hertz Fellowship. R. E. L. is grateful for funding provided by the Arnold and Mabel Beckman Foundation, 2025 Arnold O. Beckman Postdoctoral Fellowship in Chemical Instrumentation. This work was supported by a National Institutes of Health Director's New Innovator Award (DP2 GM140919-01 for L. W.), an Alfred P. Sloan Research Fellowship (L. W.), and an NSF CAREER Award (CHE-2240092 for L. W.). L. W. is a Heritage Principal Investigator supported by the Heritage Medical Research Institute at Caltech.

Notes and references

1 W. E. Moerner and L. Kador, Optical detection and spectroscopy of single molecules in a solid, *Phys. Rev. Lett.*, 1989, **62**, 2535–2538.
2 M. Orrit and J. Bernard, Single pentacene molecules detected by fluorescence excitation in a p-terphenyl crystal, *Phys. Rev. Lett.*, 1990, **65**, 2716–2719.
3 W. P. Ambrose and W. E. Moerner, Fluorescence spectroscopy and spectral diffusion of single impurity molecules in a crystal, *Nature*, 1991, **349**, 225–227.
4 M. Orrit, J. Bernard, A. Zumbusch and R. I. Personov, Stark effect on single molecules in a polymer matrix, *Chem. Phys. Lett.*, 1992, **196**, 595–600.
5 P. Tamarat, A. Maali, B. Lounis and M. Orrit, Ten Years of Single-Molecule Spectroscopy, *J. Phys. Chem. A*, 2000, **104**, 1–16.
6 W. E. Moerner and D. P. Fromm, Methods of single-molecule fluorescence spectroscopy and microscopy, *Rev. Sci. Instrum.*, 2003, **74**, 3597–3619.
7 E. Betzig and R. J. Chichester, Single molecules observed by near-field scanning optical microscopy, *Science*, 1993, **262**, 1422–1425.
8 S. A. Rosenberg, M. E. Quinlan, J. N. Forkey and Y. E. Goldman, Rotational motions of macro-molecules by single-molecule fluorescence microscopy, *Acc. Chem. Res.*, 2005, **38**, 583–593.
9 A. Yildiz, J. N. Forkey, S. A. McKinney, T. Ha, Y. E. Goldman and P. R. Selvin, Myosin V walks hand-over-hand: single fluorophore imaging with 1.5-nm localization, *Science*, 2003, **300**, 2061–2065.
10 A. D. Mehta, M. Rief, J. A. Spudich, D. A. Smith and R. M. Simmons, Single-molecule biomechanics with optical methods, *Science*, 1999, **283**, 1689–1695.
11 E. Bertrand, P. Chartrand, M. Schaefer, S. M. Shenoy, R. H. Singer and R. M. Long, Localization of ASH1 mRNA particles in living yeast, *Mol. Cell*, 1998, **2**, 437–445.
12 J. M. Levsky, S. M. Shenoy, R. C. Pezo and R. H. Singer, Single-cell gene expression profiling, *Science*, 2002, **297**, 836–840.
13 E. Betzig, G. H. Patterson, R. Sougrat, O. W. Lindwasser, S. Olenych, J. S. Bonifacino, M. W. Davidson, J. Lippincott-Schwartz and H. F. Hess, Imaging intracellular fluorescent proteins at nanometer resolution, *Science*, 2006, **313**, 1642–1645.
14 H. Noji, R. Yasuda, M. Yoshida and K. Kinosita Jr, Direct observation of the rotation of F1-ATPase, *Nature*, 1997, **386**, 299–302.
15 T. Ha, T. Enderle, D. F. Ogletree, D. S. Chemla, P. R. Selvin and S. Weiss, Probing the interaction between two single molecules: fluorescence resonance energy transfer between a single donor and a single acceptor, *Proc. Natl. Acad. Sci. U. S. A.*, 1996, **93**, 6264–6268.
16 A. A. Deniz, T. A. Laurence, G. S. Beligere, M. Dahan, A. B. Martin, D. S. Chemla, P. E. Dawson, P. G. Schultz and S. Weiss, Single-molecule protein folding: diffusion fluorescence resonance energy transfer studies of the denaturation of chymotrypsin inhibitor 2, *Proc. Natl. Acad. Sci. U. S. A.*, 2000, **97**, 5179–5184.
17 E. A. Lipman, B. Schuler, O. Bakajin and W. A. Eaton, Single-molecule measurement of protein folding kinetics, *Science*, 2003, **301**, 1233–1235.
18 M. Lelek, M. T. Gyparaki, G. Beliu, F. Schueder, J. Griffie, S. Manley, R. Jungmann, M. Sauer, M. Lakadamyali and C. Zimmer, Single-molecule localization microscopy, *Nat. Rev. Methods Primers*, 2021, **1**, 39.
19 S. C. M. Reinhardt, L. A. Masullo, I. Baudrexel, P. R. Steen, R. Kowalewski, A. S. Eklund, S. Strauss, E. M. Unterauer, T. Schlichthaerle, M. T. Strauss, C. Klein and R. Jungmann, Angstrom-resolution fluorescence microscopy, *Nature*, 2023, **617**, 711–716.
20 C. W. Freudiger, W. Min, B. G. Saar, S. Lu, G. R. Holtom, C. He, J. C. Tsai, J. X. Kang and X. S. Xie, Label-free biomedical imaging with high sensitivity by stimulated Raman scattering microscopy, *Science*, 2008, **322**, 1857–1861.
21 H. Wang, D. Lee and L. Wei, Toward the Next Frontiers of Vibrational Bioimaging, *Chem. Biomed. Imaging*, 2023, **1**, 3–17.
22 L. Wei, F. Hu, Y. Shen, Z. Chen, Y. Yu, C. C. Lin, M. C. Wang and W. Min, Live-cell imaging of alkyne-tagged small biomolecules by stimulated Raman scattering, *Nat. Methods*, 2014, **11**, 410–412.
23 H. He, J. Yin, M. Li, C. V. P. Dessai, M. Yi, X. Teng, M. Zhang, Y. Li, Z. Du, B. Xu and J. X. Cheng, Mapping enzyme activity in living systems by real-time mid-infrared photothermal imaging of nitrile chameleons, *Nat. Methods*, 2024, **21**, 342–352.
24 L. Wei, Y. Yu, Y. Shen, M. C. Wang and W. Min, Vibrational imaging of newly synthesized proteins in live cells by stimulated Raman scattering microscopy, *Proc. Natl. Acad. Sci. U. S. A.*, 2013, **110**, 11226–11231.
25 K. Miao and L. Wei, Live-Cell Imaging and Quantification of PolyQ Aggregates by Stimulated Raman Scattering of

Selective Deuterium Labeling, *ACS Cent. Sci.*, 2020, **6**, 478–486.
26 L. Wei, Z. Chen, L. Shi, R. Long, A. V. Anzalone, L. Zhang, F. Hu, R. Yuste, V. W. Cornish and W. Min, Super-multiplex vibrational imaging, *Nature*, 2017, **544**, 465–470.
27 Y. Miao, N. Qian, L. Shi, F. Hu and W. Min, 9-Cyanopyronin probe palette for super-multiplexed vibrational imaging, *Nat. Commun.*, 2021, **12**, 4518.
28 X. Bi, K. Miao and L. Wei, Alkyne-Tagged Raman Probes for Local Environmental Sensing by Hydrogen-Deuterium Exchange, *J. Am. Chem. Soc.*, 2022, **144**, 8504–8514.
29 S. D. Fried and S. G. Boxer, Measuring electric fields and noncovalent interactions using the vibrational stark effect, *Acc. Chem. Res.*, 2015, **48**, 998–1006.
30 S. H. Schneider, H. T. Kratochvil, M. T. Zanni and S. G. Boxer, Solvent-Independent Anharmonicity for Carbonyl Oscillators, *J. Phys. Chem. B*, 2017, **121**, 2331–2338.
31 J. M. Kirsh and J. Kozuch, Hydrogen Bond Blueshifts in Nitrile Vibrational Spectra Are Dictated by Hydrogen Bond Geometry and Dynamics, *JACS Au*, 2024, **4**, 4844–4855.
32 T. L. Brown, Infrared Intensities And Molecular Structure, *Chem. Rev.*, 1958, **58**, 581–608.
33 C. R. Markus, A. J. Perry, J. N. Hodges and B. J. McCall, Improving cavity-enhanced spectroscopy of molecular ions in the mid-infrared with up-conversion detection and Brewster-plate spoilers, *Opt. Express*, 2017, **25**, 3709–3721.
34 K. Huang, J. Fang, M. Yan, E. Wu and H. Zeng, Wide-field mid-infrared single-photon upconversion imaging, *Nat. Commun.*, 2022, **13**, 1077.
35 J. A. Lau, V. B. Verma, D. Schwarzer and A. M. Wodtke, Superconducting single-photon detectors in the mid-infrared for physical chemistry and spectroscopy, *Chem. Soc. Rev.*, 2023, **52**, 921–941.
36 J. N. Mastron and A. Tokmakoff, Two-Photon-Excited Fluorescence-Encoded Infrared Spectroscopy, *J. Phys. Chem. A*, 2016, **120**, 9178–9187.
37 X. Gao, N. Qian and W. Min, Principle of Stimulated Raman Scattering Microscopy: Emerging at High Spatiotemporal Limits, *J. Phys. Chem. C*, 2025, **129**, 5789–5797.
38 X. G. Xu, M. Rang, I. M. Craig and M. B. Raschke, Pushing the Sample-Size Limit of Infrared Vibrational Nanospectroscopy: From Monolayer toward Single Molecule Sensitivity, *J. Phys. Chem. Lett.*, 2012, **3**, 1836–1841.
39 J. K. Trautman and J. J. Macklin, Time-resolved spectroscopy of single molecules using near-field and far-field optics, *Chem. Phys.*, 1996, **205**, 221–229.
40 N. Qian, H. Xiong, L. Wei, L. Shi and W. Min, Merging Vibrational Spectroscopy with Fluorescence Microscopy: Combining the Best of Two Worlds, *Annu. Rev. Phys. Chem.*, 2025, **76**, 279–301.
41 A. M. Kelley, Vibrational spectroscopy of single molecules/single entities without plasmonic enhancement, *Appl. Spectrosc. Rev.*, 2025, **60**, 671–685.
42 G. Eckhardt, R. W. Hellwarth, F. J. McClung, S. E. Schwarz, D. Weiner and E. J. Woodbury, Stimulated Raman Scattering From Organic Liquids, *Phys. Rev. Lett.*, 1962, **9**, 455–457.
43 T. Yajima and M. Takatsuji, Higher Order Optical Mixing of Raman Laser Light in Nonlinear Dielectric Media, *J. Phys. Soc. Jpn.*, 1964, **19**, 2343–2344.
44 P. D. Maker and R. W. Terhune, Study of Optical Effects Due to an Induced Polarization Third Order in the Electric Field Strength, *Phys. Rev.*, 1965, **137**, A801–A818.
45 C. Zhang, D. Zhang and J. X. Cheng, Coherent Raman Scattering Microscopy in Biology and Medicine, *Annu. Rev. Biomed. Eng.*, 2015, **17**, 415–445.
46 H. Rigneault, in *Stimulated Raman Scattering Microscopy: Techniques and Applications*, ed. J.-X. Cheng, W. Min, Y. Ozeki and D. Polli, Elsevier, Amsterdam, Netherlands, 2022, pp. 3–20.
47 X. Gao and W. Min, Quantum theory of stimulated Raman scattering microscopy, *Chem. Phys. Rev.*, 2025, **6**, 021306.
48 W. Min, J.-X. Cheng and Y. Ozeki, Theory, innovations and applications of stimulated Raman scattering microscopy, *Nat. Photonics*, 2025, **19**, 803–816.
49 L. Shi, H. Xiong, Y. Shen, R. Long, L. Wei and W. Min, Electronic Resonant Stimulated Raman Scattering Micro-Spectroscopy, *J. Phys. Chem. B*, 2018, **122**, 9218–9224.
50 C. Domes, R. Domes, J. Popp, M. W. Pletz and T. Frosch, Ultrasensitive Detection of Antiseptic Antibiotics in Aqueous Media and Human Urine Using Deep UV Resonance Raman Spectroscopy, *Anal. Chem.*, 2017, **89**, 9997–10003.
51 A. B. Zrimsek, N. Chiang, M. Mattei, S. Zaleski, M. O. McAnally, C. T. Chapman, A. I. Henry, G. C. Schatz and R. P. Van Duyne, Single-Molecule Chemistry with Surface- and Tip-Enhanced Raman Spectroscopy, *Chem. Rev.*, 2017, **117**, 7583–7613.
52 E. J. Blackie, E. C. Le Ru and P. G. Etchegoin, Single-molecule surface-enhanced Raman spectroscopy of nonresonant molecules, *J. Am. Chem. Soc.*, 2009, **131**, 14466–14472.
53 K. Kneipp, Y. Wang, H. Kneipp, L. T. Perelman, I. Itzkan, R. R. Dasari and M. S. Feld, Single Molecule Detection Using Surface-Enhanced Raman Scattering (SERS), *Phys. Rev. Lett.*, 1997, **78**, 1667–1670.
54 S. Nie and S. R. Emory, Probing Single Molecules and Single Nanoparticles by Surface-Enhanced Raman Scattering, *Science*, 1997, **275**, 1102–1106.
55 W. Zhang, B. S. Yeo, T. Schmid and R. Zenobi, Single Molecule Tip-Enhanced Raman Spectroscopy with Silver Tips, *J. Phys. Chem. C*, 2007, **111**, 1733–1738.
56 P. G. Etchegoin and E. C. Le Ru, Resolving single molecules in surface-enhanced Raman scattering within the inhomogeneous broadening of Raman peaks, *Anal. Chem.*, 2010, **82**, 2888–2892.
57 Z. He, W. Qiu, M. E. Kizer, J. Wang, W. Chen, A. V. Sokolov, X. Wang, J. Hu and M. O. Scully, Resolving the Sequence of RNA Strands by Tip-Enhanced Raman Spectroscopy, *ACS Photonics*, 2021, **8**, 424–430.
58 T. W. Koo, S. Chan and A. A. Berlin, Single-molecule detection of biomolecules by surface-enhanced coherent

anti-Stokes Raman scattering, *Opt. Lett.*, 2005, **30**, 1024–1026.
59 C. K. Chen, A. R. B. de Castro, Y. R. Shen and F. DeMartini, Surface Coherent Anti-Stokes Raman Spectroscopy, *Phys. Rev. Lett.*, 1979, **43**, 946–949.
60 Y. Zhang, Y. R. Zhen, O. Neumann, J. K. Day, P. Nordlander and N. J. Halas, Coherent anti-Stokes Raman scattering with single-molecule sensitivity using a plasmonic Fano resonance, *Nat. Commun.*, 2014, **5**, 4424.
61 S. Yampolsky, D. A. Fishman, S. Dey, E. Hulkko, M. Banik, E. O. Potma and V. A. Apkarian, Seeing a single molecule vibrate through time-resolved coherent anti-Stokes Raman scattering, *Nat. Photonics*, 2014, **8**, 650–656.
62 C. Zong, R. Premasiri, H. Lin, Y. Huang, C. Zhang, C. Yang, B. Ren, L. D. Ziegler and J. X. Cheng, Plasmon-enhanced stimulated Raman scattering microscopy with single-molecule detection sensitivity, *Nat. Commun.*, 2019, **10**, 5318.
63 J. Du, X. Tao, T. Begusic and L. Wei, Computational Design of Molecular Probes for Electronic Preresonance Raman Scattering Microscopy, *J. Phys. Chem. B*, 2023, **127**, 4979–4988.
64 K. Ataka, S. T. Stripp and J. Heberle, Surface-enhanced infrared absorption spectroscopy (SEIRAS) to probe monolayers of membrane proteins, *Biochim. Biophys. Acta*, 2013, **1828**, 2283–2293.
65 F. Neubrech, A. Pucci, T. W. Cornelius, S. Karim, A. Garcia-Etxarri and J. Aizpurua, Resonant plasmonic and vibrational coupling in a tailored nanoantenna for infrared detection, *Phys. Rev. Lett.*, 2008, **101**, 157403.
66 T. Tanaka, T. A. Yano and R. Kato, Nanostructure-enhanced infrared spectroscopy, *Nanophotonics*, 2022, **11**, 2541–2561.
67 E. A. Muller, B. Pollard and M. B. Raschke, Infrared Chemical Nano-Imaging: Accessing Structure, Coupling, and Dynamics on Molecular Length Scales, *J. Phys. Chem. Lett.*, 2015, **6**, 1275–1284.
68 B. J. Bjork, T. Q. Bui, O. H. Heckl, P. B. Changala, B. Spaun, P. Heu, D. Follman, C. Deutsch, G. D. Cole, M. Aspelmeyer, M. Okumura and J. Ye, Direct frequency comb measurement of OD + CO -> DOCO kinetics, *Science*, 2016, **354**, 444–448.
69 C. R. Markus, J. Hayden, D. I. Herman, P. A. Kocheril, D. C. Ober, T. Bashiri, M. Mangold and M. Okumura, Cavity-enhanced dual-comb spectroscopy in the molecular fingerprint region using free-running quantum cascade lasers, *J. Opt. Soc. Am. B*, 2024, **41**, E56–E64.
70 L. M. Needham, C. Saavedra, J. K. Rasch, D. Sole-Barber, B. S. Schweitzer, A. J. Fairhall, C. H. Vollbrecht, S. Wan, Y. Podorova, A. J. Bergsten, B. Mehlenbacher, Z. Zhang, L. Tenbrake, J. Saimi, L. C. Kneely, J. S. Kirkwood, H. Pfeifer, E. R. Chapman and R. H. Goldsmith, Label-free detection and profiling of individual solution-phase molecules, *Nature*, 2024, **629**, 1062–1068.
71 F. Benz, M. K. Schmidt, A. Dreismann, R. Chikkaraddy, Y. Zhang, A. Demetriadou, C. Carnegie, H. Ohadi, B. de Nijs, R. Esteban, J. Aizpurua and J. J. Baumberg, Single-molecule optomechanics in "picocavities", *Science*, 2016, **354**, 726–729.
72 L. J. G. W. van Wilderen, A. T. Messmer and J. Bredenbeck, Mixed IR/Vis two-dimensional spectroscopy: chemical exchange beyond the vibrational lifetime and sub-ensemble selective photochemistry, *Angew. Chem., Int. Ed.*, 2014, **53**, 2667–2672.
73 A. Calvin, S. Eierman, Z. Peng, M. Brzeczek, L. Satterthwaite and D. Patterson, Single molecule infrared spectroscopy in the gas phase, *Nature*, 2023, **621**, 295–299.
74 G. A. West, J. J. Barrett, D. R. Siebert and K. V. Reddy, Photoacoustic spectroscopy, *Rev. Sci. Instrum.*, 1983, **54**, 797–817.
75 T. M. Nguyen, D. C. Ober, A. Balaji, F. W. Maiwald, R. P. Hodyss, S. M. Madzunkov, M. Okumura and D. J. Nemchick, Infrared Photodissociation Spectroscopy of Water-Tagged Ions with a Widely Tunable Quantum Cascade Laser for Planetary Science Applications, *Anal. Chem.*, 2024, **96**, 8875–8879.
76 M. Sakai, Vibrational Energy Relaxation Process of the 7-Azaindole Dimer in Gas Phase and Solution, *Bunko Kenkyu*, 2005, **54**, 163–169.
77 P. G. Kryukov, V. S. Letokhov, Y. A. Matveets, D. N. Nikogosyan and A. V. Sharkov, Selective two-stage excitation of an electronic state of organic molecules in aqueous solution by picosecond light pulse, *Sov. J. Quantum Electron.*, 1978, **8**, 1405–1407.
78 M. Sakai and M. Fujii, Vibrational energy relaxation of the 7-azaindole dimer in CCl4 solution studied by picosecond time-resolved transient fluorescence detected IR spectroscopy, *Chem. Phys. Lett.*, 2004, **396**, 298–302.
79 N. P. Gallop, D. R. Maslennikov, N. Mondal, K. P. Goetz, Z. Dai, A. M. Schankler, W. Sung, S. Nihonyanagi, T. Tahara, M. I. Bodnarchuk, M. V. Kovalenko, Y. Vaynzof, A. M. Rappe and A. A. Bakulin, Ultrafast vibrational control of organohalide perovskite optoelectronic devices using vibrationally promoted electronic resonance, *Nat. Mater.*, 2024, **23**, 88–94.
80 T. Tamura, P. C. McCann, R. Nishiyama, K. Hiramatsu and K. Goda, Fluorescence-Encoded Time-Domain Coherent Raman Spectroscopy in the Visible Range, *J. Phys. Chem. Lett.*, 2024, **15**, 4940–4947.
81 A. Xomalis, X. Zheng, R. Chikkaraddy, Z. Koczor-Benda, E. Miele, E. Rosta, G. A. E. Vandenbosch, A. Martinez and J. J. Baumberg, Detecting mid-infrared light by molecular frequency upconversion in dual-wavelength nanoantennas, *Science*, 2021, **374**, 1268–1271.
82 R. Chikkaraddy, R. Arul, L. A. Jakob and J. J. Baumberg, Single-molecule mid-infrared spectroscopy and detection through vibrationally assisted luminescence, *Nat. Photonics*, 2023, **17**, 865–871.
83 A. Gaiduk, M. Yorulmaz, P. V. Ruijgrok and M. Orrit, Room-temperature detection of a single molecule's absorption by photothermal contrast, *Science*, 2010, **330**, 353–356.
84 M. Celebrano, P. Kukura, A. Renn and V. Sandoghdar, Single-molecule imaging by optical absorption, *Nat. Photonics*, 2011, **5**, 95–98.

85 B. C. Stipe, M. A. Rezaei and W. Ho, Single-molecule vibrational spectroscopy and microscopy, *Science*, 1998, **280**, 1732–1735.
86 R. C. Jaklevic and J. Lambe, Molecular Vibration Spectra by Electron Tunneling, *Phys. Rev. Lett.*, 1966, **17**, 1139–1140.
87 W. Ho, Single-molecule chemistry, *J. Chem. Phys.*, 2002, **117**, 11033–11061.
88 A. Laubereau, A. Seilmeier and W. Kaiser, A new technique to measure ultrashort vibrational relaxation times in liquid systems, *Chem. Phys. Lett.*, 1975, **36**, 232–237.
89 A. Centrone, Infrared Imaging and Spectroscopy Beyond the Diffraction Limit, *Annu. Rev. Anal. Chem.*, 2015, **8**, 101–126.
90 F. S. Ruggeri, B. Mannini, R. Schmid, M. Vendruscolo and T. P. J. Knowles, Single molecule secondary structure determination of proteins through infrared absorption nanospectroscopy, *Nat. Commun.*, 2020, **11**, 2945.
91 D. Zhang, C. Li, C. Zhang, M. N. Slipchenko, G. Eakins and J. X. Cheng, Depth-resolved mid-infrared photothermal imaging of living cells and organisms with submicrometer spatial resolution, *Sci. Adv.*, 2016, **2**, e1600521.
92 Y. Bai, J. Yin and J. X. Cheng, Bond-selective imaging by optically sensing the mid-infrared photothermal effect, *Sci. Adv.*, 2021, **7**, eabg1559.
93 Y. Zhu, X. Ge, H. Ni, J. Yin, H. Lin, L. Wang, Y. Tan, C. V. P. Dessai, Y. Li, X. Teng and J. X. Cheng, Stimulated Raman photothermal microscopy toward ultrasensitive chemical imaging, *Sci. Adv.*, 2023, **9**, eadi2181.
94 L. Wang, H. Lin, Y. Zhu, X. Ge, M. Li, J. Liu, F. Chen, M. Zhang and J. X. Cheng, Overtone photothermal microscopy for high-resolution and high-sensitivity vibrational imaging, *Nat. Commun.*, 2024, **15**, 5374.
95 H. Ni, Y. Yuan, M. Li, Y. Zhu, X. Ge, J. Yin, C. P. Dessai, L. Wang and J. X. Cheng, Millimetre-deep micrometre-resolution vibrational imaging by shortwave infrared photothermal microscopy, *Nat. Photonics*, 2024, **18**, 944–951.
96 P. Fu, Y. Zhang, S. Wang, X. Ye, Y. Wu, M. Yu, S. Zhu, H. J. Lee and D. Zhang, INSPIRE: Single-beam probed complementary vibrational bioimaging, *Sci. Adv.*, 2024, **10**, eadm7687.
97 D. Jia, R. Cheng, J. H. McNeely, H. Zong, X. Teng, X. Xu and J. X. Cheng, Ultrasensitive infrared spectroscopy via vibrational modulation of plasmonic scattering from a nanocavity, *Sci. Adv.*, 2024, **10**, eadn8255.
98 M. Li, A. Razumtcev, R. Yang, Y. Liu, J. Rong, A. C. Geiger, R. Blanchard, C. Pfluegl, L. S. Taylor and G. J. Simpson, Fluorescence-Detected Mid-Infrared Photothermal Microscopy, *J. Am. Chem. Soc.*, 2021, **143**, 10809–10815.
99 Y. Zhang, H. Zong, C. Zong, Y. Tan, M. Zhang, Y. Zhan and J. X. Cheng, Fluorescence-Detected Mid-Infrared Photothermal Microscopy, *J. Am. Chem. Soc.*, 2021, **143**, 11490–11499.
100 K. Otomo, T. Dewa, M. Matsushita and S. Fujiyoshi, Cryogenic Single-Molecule Fluorescence Detection of the Mid-Infrared Response of an Intrinsic Pigment in a Light-Harvesting Complex, *J. Phys. Chem. B*, 2023, **127**, 4959–4965.
101 A. Laubereau and W. Kaiser, Vibrational Dynamics of Liquids and Solids Investigated by Picosecond Light Pulses, *Rev. Mod. Phys.*, 1978, **50**, 607–665.
102 J. P. Maier, A. Seilmeier and W. Kaiser, Population lifetime of CH-stretching modes in medium-size molecules, *Chem. Phys. Lett.*, 1980, **70**, 591–596.
103 F. Wondrazek, A. Seilmeier and W. Kaiser, Ultrafast intramolecular redistribution and intermolecular relaxation of vibrational energy in large molecules, *Chem. Phys. Lett.*, 1984, **104**, 121–128.
104 A. Seilmeier and W. Kaiser, in *Ultrashort Laser Pulses and Applications*, ed. W. Kaiser, Springer Berlin, Heidelberg, 1988, ch. 7, pp. 279–317.
105 A. Seilmeier, W. Kaiser, A. Laubereau and S. F. Fischer, A novel spectroscopy using ultrafast two-pulse excitation of large polyatomic molecules, *Chem. Phys. Lett.*, 1978, **58**, 225–229.
106 T. Dahinten, J. Baier and A. Seilmeier, Vibrational energy transfer processes in dye molecules after ultrafast excitation of skeletal modes, *Chem. Phys.*, 1998, **232**, 239–245.
107 J. C. Wright, Double Resonance Excitation of Fluorescence in the Condensed Phase—An Alternative to Infrared, Raman, and Fluorescence Spectroscopy, *Appl. Spectrosc.*, 1980, **34**, 151–157.
108 S. H. Lee, D. C. Nguyen and J. C. Wright, Double Resonance Excitation of Fluorescence by Stimulated Raman Scattering, *Appl. Spectrosc.*, 1983, **37**, 472–474.
109 M. J. Winterhalder, A. Zumbusch, M. Lippitz and M. Orrit, Toward far-field vibrational spectroscopy of single molecules at room temperature, *J. Phys. Chem. B*, 2011, **115**, 5425–5430.
110 M. Sakai, Y. Kawashima, A. Takeda, T. Ohmori and M. Fujii, Far-field infrared super-resolution microscopy using picosecond time-resolved transient fluorescence detected IR spectroscopy, *Chem. Phys. Lett.*, 2007, **439**, 171–176.
111 N. Bokor, K. Inoue, S. Kogure, M. Fujii and M. Sakai, Visible-super-resolution infrared microscopy using saturated transient fluorescence detected infrared spectroscopy, *Opt. Commun.*, 2010, **283**, 509–514.
112 H. Takahashi, T. Oue and M. Sakai, Resonance IR spectroscopy in aqueous solution by combining IR super-resolution with TFD-IR method, *Chem. Phys. Lett.*, 2020, **758**, 137942.
113 J. N. Mastron and A. Tokmakoff, Fourier Transform Fluorescence-Encoded Infrared Spectroscopy, *J. Phys. Chem. A*, 2018, **122**, 554–562.
114 Y. Qiu, C. Kuang, X. Liu and L. Tang, Single-Molecule Surface-Enhanced Raman Spectroscopy, *Sensors*, 2022, **22**, 4889.
115 H. Xiong, L. Shi, L. Wei, Y. Shen, R. Long, Z. Zhao and W. Min, Stimulated Raman Excited Fluorescence Spectroscopy and Imaging, *Nat. Photonics*, 2019, **13**, 412–417.

116 H. Xiong and W. Min, Combining the best of two worlds: Stimulated Raman excited fluorescence, *J. Chem. Phys.*, 2020, **153**, 210901.
117 L. Shi, F. Hu and W. Min, Optical mapping of biological water in single live cells by stimulated Raman excited fluorescence microscopy, *Nat. Commun.*, 2019, **10**, 4764.
118 H. Xiong, J. K. Lee, R. N. Zare and W. Min, Strong Electric Field Observed at the Interface of Aqueous Microdroplets, *J. Phys. Chem. Lett.*, 2020, **11**, 7423–7428.
119 H. Xiong, N. Qian, Y. Miao, Z. Zhao, C. Chen and W. Min, Super-resolution vibrational microscopy by stimulated Raman excited fluorescence, *Light:Sci. Appl.*, 2021, **10**, 87.
120 Q. Yu, Z. Yao, H. Zhang, Z. Li, Z. Chen and H. Xiong, Transient Stimulated Raman Excited Fluorescence Spectroscopy, *J. Am. Chem. Soc.*, 2023, **145**, 7758–7762.
121 L. Whaley-Mayda, S. B. Penwell and A. Tokmakoff, Fluorescence-Encoded Infrared Spectroscopy: Ultrafast Vibrational Spectroscopy on Small Ensembles of Molecules in Solution, *J. Phys. Chem. Lett.*, 2019, **10**, 1967–1972.
122 L. Whaley-Mayda, A. Guha, S. B. Penwell and A. Tokmakoff, Fluorescence-Encoded Infrared Vibrational Spectroscopy with Single-Molecule Sensitivity, *J. Am. Chem. Soc.*, 2021, **143**, 3060–3064.
123 L. Whaley-Mayda, A. Guha and A. Tokmakoff, Resonance conditions, detection quality, and single-molecule sensitivity in fluorescence-encoded infrared vibrational spectroscopy, *J. Chem. Phys.*, 2022, **156**, 174202.
124 L. Whaley-Mayda, A. Guha and A. Tokmakoff, Multimode vibrational dynamics and orientational effects in fluorescence-encoded infrared spectroscopy. I. Response function theory, *J. Chem. Phys.*, 2023, **159**, 194201.
125 L. Whaley-Mayda, A. Guha and A. Tokmakoff, Multimode vibrational dynamics and orientational effects in fluorescence-encoded infrared spectroscopy. II. Analysis of early-time signals, *J. Chem. Phys.*, 2023, **159**, 194202.
126 A. Guha, L. Whaley-Mayda, S. Y. Lee and A. Tokmakoff, Molecular factors determining brightness in fluorescence-encoded infrared vibrational spectroscopy, *J. Chem. Phys.*, 2024, **160**, 104202.
127 H. Wang, D. Lee, Y. Cao, X. Bi, J. Du, K. Miao and L. Wei, Bond-selective fluorescence imaging with single-molecule sensitivity, *Nat. Photonics*, 2023, **17**, 846–855.
128 P. A. Kocheril, H. Wang, D. Lee, N. Naji and L. Wei, Nitrile Vibrational Lifetimes as Probes of Local Electric Fields, *J. Phys. Chem. Lett.*, 2024, **15**, 5306–5314.
129 P. A. Kocheril, J. Du, H. Wang, R. E. Leighton, D. Lee, Z. Yang, N. Naji, A. Colazo and L. Wei, Two-dimensional bond-selective fluorescence spectroscopy: violations of the resonance condition, vibrational cooling rate dispersion, and super-multiplex imaging, *Chem. Sci.*, 2025, **16**, 14905–14918.
130 D. Lee, H. Wang, P. A. Kocheril, X. Bi, N. Naji and L. Wei, Wide-field bond-selective fluorescence imaging: from single-molecule to cellular imaging beyond video rate, *Optica*, 2025, **12**, 148–157.
131 H. Wang, P. A. Kocheril, Z. Yang, D. Lee, N. Naji, J. Du, L. E. Lin and L. Wei, Room-Temperature Single-Molecule Infrared Imaging and Spectroscopy through Bond-Selective Fluorescence, *Angew. Chem., Int. Ed.*, 2024, **63**, e202413647.
132 C. Yan, C. Wang, J. C. Wagner, J. Ren, C. Lee, Y. Wan, S. E. Wang and W. Xiong, Multidimensional Widefield Infrared-Encoded Spontaneous Emission Microscopy: Distinguishing Chromophores by Ultrashort Infrared Pulses, *J. Am. Chem. Soc.*, 2024, **146**, 1874–1886.
133 Q. Yu, X. Li, C. Shen, Z. Yu, J. Guan and J. Zheng, Blue-Shifted and Broadened Fluorescence Enhancement by Visible and Mode-Selective Infrared Double Excitations, *J. Phys. Chem. A*, 2024, **128**, 2912–2922.
134 Q. Yu, X. Li, C. Shen, Z. Yu, J. Guan and J. Zheng, Direct observation of long-lived vibrational hot ground states by ultrafast spectroscopy and visible/lnfrared double excitation fluorescence, *Chin. J. Chem. Phys.*, 2024, **37**, 411–419.
135 J. Guan, X. Li, C. Shen, Z. Zi, Z. Hou, C. Hao, Q. Yu, H. Jiang, Y. Ma, Z. Yu and J. Zheng, Vibrational-Mode-Selective Modulation of Electronic Excitation, *ChemPhysChem*, 2024, **25**, e202400335.
136 Z. D. Meng, T. R. Wu, L. L. Zhou, E. M. You, Z. P. Dong, X. G. Zhang, G. Y. Chen, D. Y. Wu, J. Yi and Z. Q. Tian, Colocalized Raman and IR Spectroscopies via Vibrational-Encoded Fluorescence for Comprehensive Vibrational Analysis, *J. Am. Chem. Soc.*, 2025, **147**, 16309–16318.
137 J. Zhou, B. Del Rosal, D. Jaque, S. Uchiyama and D. Jin, Advances and challenges for fluorescence nanothermometry, *Nat. Methods*, 2020, **17**, 967–980.
138 B. Figueroa, R. Hu, S. G. Rayner, Y. Zheng and D. Fu, Real-Time Microscale Temperature Imaging by Stimulated Raman Scattering, *J. Phys. Chem. Lett.*, 2020, **11**, 7083–7089.
139 P. A. Kocheril, D. Lee, N. Naji, R. S. Chadha, R. E. Leighton, H. Wang and L. Wei, Single-Molecule Vibrational Thermometry, *J. Phys. Chem. B*, 2025, **129**, 8788–8797.
140 S. D. Fried, S. Bagchi and S. G. Boxer, Extreme electric fields power catalysis in the active site of ketosteroid isomerase, *Science*, 2014, **346**, 1510–1514.
141 S. Ye, A. P. Latham, Y. Tang, C. H. Hsiung, J. Chen, F. Luo, Y. Liu, B. Zhang and X. Zhang, Micropolarity governs the structural organization of biomolecular condensates, *Nat. Chem. Biol.*, 2024, **20**, 443–451.
142 S. F. Banani, H. O. Lee, A. A. Hyman and M. K. Rosen, Biomolecular condensates: organizers of cellular biochemistry, *Nat. Rev. Mol. Cell Biol.*, 2017, **18**, 285–298.
143 M. H. Hicks, W. Nie, A. E. Boehme, H. A. Atwater, T. Agapie and J. C. Peters, Electrochemical CO(2) Reduction in Acidic Electrolytes: Spectroscopic Evidence for Local pH Gradients, *J. Am. Chem. Soc.*, 2024, **146**, 25282–25289.
144 H. Xiong, N. Qian, Y. Miao, Z. Zhao and W. Min, Stimulated Raman Excited Fluorescence Spectroscopy of Visible Dyes, *J. Phys. Chem. Lett.*, 2019, **10**, 3563–3570.
145 P. Shieh, V. T. Dien, B. J. Beahm, J. M. Castellano, T. Wyss-Coray and C. R. Bertozzi, CalFluors: A Universal Motif for

Fluorogenic Azide Probes across the Visible Spectrum, *J. Am. Chem. Soc.*, 2015, **137**, 7145–7151.

146 G. Lee, D. Kossowska, J. Lim, S. Kim, H. Han, K. Kwak and M. Cho, Cyanamide as an Infrared Reporter: Comparison of Vibrational Properties between Nitriles Bonded to N and C Atoms, *J. Phys. Chem. B*, 2018, **122**, 4035–4044.

147 J. Kubel, G. Lee, S. A. Ooi, S. Westenhoff, H. Han, M. Cho and M. Maj, Ultrafast Chemical Exchange Dynamics of Hydrogen Bonds Observed via Isonitrile Infrared Sensors: Implications for Biomolecular Studies, *J. Phys. Chem. Lett.*, 2019, **10**, 7878–7883.

148 T. B. Grindley, K. F. Johnson, A. R. Katritzky, H. J. Keogh, C. Thirkettle, R. T. C. Brownlee, J. A. Munday and R. D. Topsom, Infrared intensities as a quantitative measure of intramolecular interactions. Part XXXII. Conjugation of the substituent and the triple bond in monosubstituted acetylenes, *J. Chem. Soc., Perkin Trans. 2*, 1974, 276–282.

149 S. Choi, J. Park, K. Kwak and M. Cho, Substituent Effects on the Vibrational Properties of the CN Stretch Mode of Aromatic Nitriles: IR Probes Useful for Time-resolved IR Spectroscopy, *Chem.–Asian J.*, 2021, **16**, 2626–2632.

150 N. Bloembergen and A. H. Zewail, Energy Redistribution In Isolated Molecules and the Question of Mode-Selective Laser Chemistry Revisited, *J. Phys. Chem.*, 1984, **88**, 5459–5465.

151 B. Xiang, R. F. Ribeiro, M. Du, L. Chen, Z. Yang, J. Wang, J. Yuen-Zhou and W. Xiong, Intermolecular vibrational energy transfer enabled by microcavity strong light-matter coupling, *Science*, 2020, **368**, 665–667.

152 A. P. Fidler, L. Chen, A. M. McKillop and M. L. Weichman, Ultrafast dynamics of CN radical reactions with chloroform solvent under vibrational strong coupling, *J. Chem. Phys.*, 2023, **159**, 164302.

153 A. D. Wright, J. C. Nelson and M. L. Weichman, Rovibrational Polaritons in Gas-Phase Methane, *J. Am. Chem. Soc.*, 2023, **145**, 5982–5987.

154 L. J. G. W. van Wilderen, D. Kern-Michler, C. Neumann, M. Reinfelds, J. von Cosel, M. Horz, I. Burghardt, A. Heckel and J. Bredenbeck, Choose your leaving group: selective photodeprotection in a mixture of pHP-caged compounds by VIPER excitation, *Chem. Sci.*, 2023, **14**, 2624–2630.

155 A. L. Pace, F. Xu, W. Liu, M. N. Lavagnino and D. W. C. MacMillan, Iron-Catalyzed Cross-Electrophile Coupling for the Formation of All-Carbon Quaternary Centers, *J. Am. Chem. Soc.*, 2024, **146**, 32925–32932.

156 E. R. Welin, C. Le, D. M. Arias-Rotondo, J. K. McCusker and D. W. C. MacMillan, Photosensitized, energy transfer-mediated organometallic catalysis through electronically excited nickel(II), *Science*, 2017, **355**, 380–385.

157 F. Schueder, F. Rivera-Molina, M. Su, Z. Marin, P. Kidd, J. E. Rothman, D. Toomre and J. Bewersdorf, Unraveling cellular complexity with transient adapters in highly multiplexed super-resolution imaging, *Cell*, 2024, **187**, 1769–1784.

158 E. M. Unterauer, S. S. Boushehri, K. Jevdokimenko, L. A. Masullo, M. Ganji, S. Sograte-Idrissi, R. Kowalewski, S. Strauss, S. C. M. Reinhardt, A. Perovic, C. Marr, F. Opazo, E. F. Fornasiero and R. Jungmann, Spatial proteomics in neurons at single-protein resolution, *Cell*, 2024, **187**, 1785–1800.

159 R. Heintzmann and T. Huser, Super-Resolution Structured Illumination Microscopy, *Chem. Rev.*, 2017, **117**, 13890–13908.

160 L. Gong, S. Lin and Z. Huang, Super-resolution stimulated Raman scattering microscopy enhanced by quantum light and deconvolution, *Opt. Lett.*, 2023, **48**, 6516–6519.

161 L. Mockl, A. R. Roy, P. N. Petrov and W. E. Moerner, Accurate and rapid background estimation in single-molecule localization microscopy using the deep neural network BGnet, *Proc. Natl. Acad. Sci. U. S. A.*, 2020, **117**, 60–67.